

Isotopically Labelled MGO as a Tool for the Mechanistic Study of Glycation

A Senior Honors Thesis

By

Stefan Hansel

Department of Chemistry

Tufts University

May 2, 2023

Acknowledgements

Before I begin, I'd like to thank all the people that have come together to make this project possible. First, I'd like to thank my committee members, Professor Rebecca Scheck and Professor Krishna Kumar, who have helped guide me not only through this project, but in their classes and career. In particular, Professor Scheck has consistently been there to foster my growth from an inexperienced undergraduate to a (more) developed researcher. I am forever thankful that she reached back out after COVID to offer me a spot in the lab, which has set me on such an amazing path for my career.

I'd like to thank all the members of the Scheck Lab, who have taught me even more about what graduate level researcher looks like, while also being an incredibly welcoming and fun group of people. Lab work is just much more enjoyable due to the environment they create. I would like to especially thank Tin Pham for teaching me almost everything I know about the field of glycation, including how to even perform the reaction.

I'd like to thank Professor Clay Bennett and the members of the Bennett Lab for providing me with their lab space and knowledge, which have been invaluable in my growth as a partly organic chemist. In particular, Katie Maiello has been a massive help at the beginning of my project, and taught almost everything I know about organic lab practices. This project would not have gotten past the drawing board without her.

Finally, I'd like to acknowledge the funding and support from NIH R01GM132422 and the Beckman Scholars Program. Thank you to Professor Yu-Shan Lin for organizing the Beckman Scholars program, and her work in providing us scholars with the best experience possible.

TABLE OF CONTENTS

1) Acknowledgements	2
2) Abstract	4
3) Introduction	5
3.1) <i>The Maillard Reaction and Glycation</i>	5
3.2) <i>Methylglyoxal's role in Glycation</i>	5
3.3) <i>Recent Discoveries in the Field of Glycation</i>	6
3.4) <i>Gaps in Glycation Knowledge</i>	7
3.5) <i>Experimental Design</i>	8
3.6) <i>Difficulties in MGO Synthesis</i>	9
3.7) <i>Synthetic Strategies</i>	10
4) Results	12
4.1) <i>Preliminary Riley Oxidation Results</i>	12
4.2) <i>Riley Oxidation Without p-Dioxane</i>	13
4.3) <i>Glycation Using Synthesized MGO</i>	15
4.4) <i>Purity of Commercial MGO</i>	16
4.5) <i>Correcting Synthesized MGO Concentration</i>	17
4.6) <i>Glycation After Concentration Correction</i>	18
4.7) <i>Tautomerization with Purification</i>	19
4.8) <i>Tautomerization without Purification</i>	22
4.9) <i>d4-MGO Synthesis</i>	23
4.10) <i>Glycation Using Deuterated MGO</i>	26
5) Discussion	26
6) Conclusion	30
7) Methods	31
8) References	35
9) Appendix	37

2. Abstract

Sugars and sugar derivatives in the body are known to react spontaneously with amino and guanidino groups on proteins in a process known as glycation. This nonenzymatic, post-translational modification process forms a variety of advanced glycation end-products (AGEs). Though glycation is implicated in many relevant diseases, the role of glycation in the body and the chemistry behind the process is not well understood, due to a lack of tools to study this nonenzymatic reaction. This study aimed to isotopically label the biologically-relevant glycating agent methylglyoxal (MGO) as a tool to study the mechanisms behind the formation of different AGEs. Through Riley oxidation and tautomerization under acidic conditions, it is possible to synthesize MGO that is selectively deuterated at either its methyl or aldehydic position. These isotopically-labeled positions can then be tracked as different AGEs are formed, giving insight into AGE formation mechanisms.

In this study, the Riley Oxidation procedure was successfully optimized, producing pure MGO of greater purity than commercial sources of MGO. It was also used to prepare fully deuterated MGO (d4-MGO) starting from d6-acetone. Additionally, acid-promoted tautomerization reactions have been optimized for use in the synthesis of selectively deuterated MGO (d1-MGO and d3-MGO). Meanwhile, glycation reactions using d4-MGO have helped validate a mechanism between AGEs proposed by previous work in the Scheck lab, as it has enabled us to distinguish the two isomeric AGEs of this proposed mechanism, MGH-DH and CEA. By helping to differentiate any AGEs originally of the same mass shift, deuterated MGO has already begun to inform the field of glycation. Future work will synthesize d1-MGO and d3-MGO for analysis of isomeric AGEs with mass $[M+144]$, as only one structure of these AGEs is currently known. Additionally, the mechanism of APY formation will be analyzed, as the currently accepted mechanism is chemically unrealistic.

3. Introduction

The Maillard Reaction and Glycation

The browning reaction has been shrouded in mystery since the first reports of its products were published in 1912 by Louis Maillard.¹ Maillard had stumbled upon a reaction between peptides and sugars, and hypothesized it could explain the browning of meats when cooked. However, it took another 40 years before the structures formed from this reaction were characterized by John Hodge, who began to elucidate the chemical steps that lead to the formation of these structures.² Since then, it took another 30 years to connect that same chemistry to reactions occurring between the sugars and proteins in our bodies, which had been previously referred to as non-enzymatic glycosylation.³ To christen this connection between the Maillard reaction and this *in vivo* process, it was given the name of “glycation” in order to differentiate it from its enzymatic counterpart.^{4,5} In glycation, a sugar or sugar-derived metabolite covalently attaches to amino or guanidino groups on the protein residues, such as lysine or arginine. These permanent attachments may then go through further rearrangements, resulting in the formation of many different Advanced Glycation End-products (AGEs). These AGEs are unique in structure, depending on the beginning sugar metabolite and residue involved in the process. This research focused on the AGEs formed through the interaction of arginine residues and a potent glycating agent named methylglyoxal.

Methylglyoxal's Role in Glycation

Methylglyoxal (MGO) is a highly biologically-relevant glycating agent that forms as a by-product during glycolysis. Through the elimination of the phosphate group of DHAP,⁶ MGO accumulates in cells of all types. In order to metabolize this molecule, cells in the body upkeep a glyoxalase system, which employs catalytic glutathione in order to form D-Lactate from MGO.⁷ Other glyoxalase enzymes, such as DJ-1, have also evolved to perform this same removal of

MGO even without the glutathione cofactor, such is the importance of removing MGO.⁸ This system keeps MGO concentrations at around 100 nM in blood plasma, while reaching 1-2 μM in some cell types, such as the lens, and even upward of 300 μM in Chinese hamster ovary cells.^{9,10}

MGO forms a variety of AGEs when it reacts with arginine residues, which are easily recognized by the shift in mass of the arginine due to the formation of the AGE. Some AGE structures have previously been characterized (Fig. 1). Many of these AGEs, though different in structure, have identical mass shifts when analyzed through mass spectrometry, such as the three methylglyoxal-derived hydroimidazolone isomers (MGH-1, MGH-2, and MGH-3) with a shift of [M+54], as well as MGH-DH and CEA that have a mass shift of [M+72]. The presence of these isomeric AGEs adds another layer of complexity to the study of glycation, as these AGEs must first be differentiated before they can be analyzed.

Recent Discoveries in the Field of Glycation

Previous work in the Scheck Lab has begun to suggest and support mechanisms behind the formation of some of these AGEs.¹¹ McEwen *et al.* were the among the first to propose and experimentally prove that AGEs can form as rearrangements from each other. In their study, they

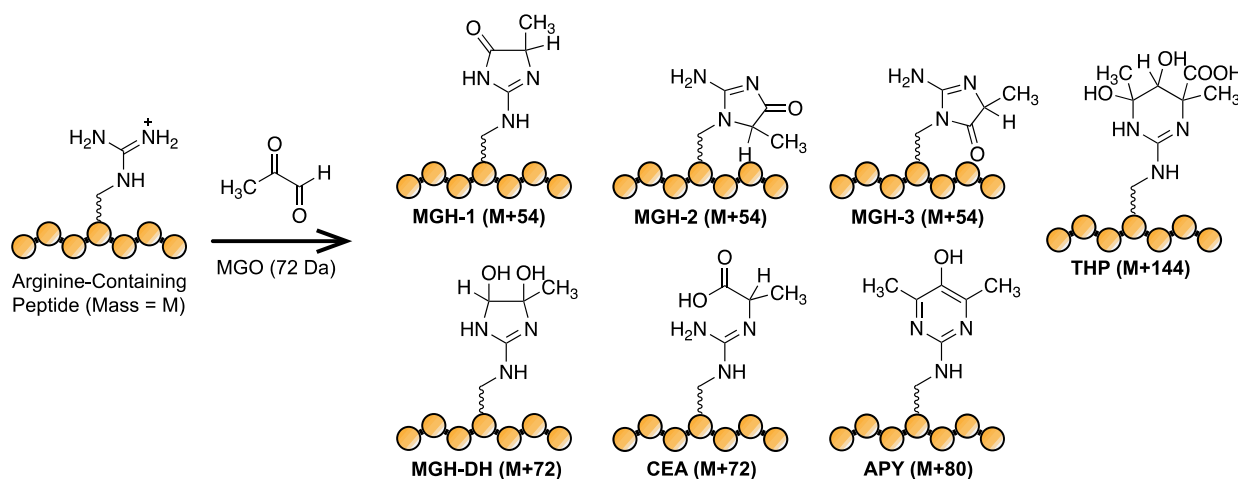


Figure 1. Current Structural Understanding of MGO Glycation. These AGEs are formed when peptide or protein of original mass "M" reacts with MGO of an original mass of 72 Da. Each AGE is identified with a unique name and the mass shift that can be observed when it forms on peptide or protein.

noticed that an [M+72] AGE was the predominant AGE at the beginning of glycation reactions, but as time went on, an [M+54] began to dominate. Using a boronic acid assay that binds to MGH-DH, but not the CEA, they determined that MGH-DH was the initial product of glycation in these rearrangements of AGEs. Through NMR, MGH-1 was determined to be the dominant AGE over time. The group then hypothesized that an elimination and tautomerization mechanism could occur to form MGH-1 from MGH-DH (Fig. 2). To test this, the authors began to dilute glycation experiments after initial glycation took place, effectively removing MGO from the reaction. This meant that any new AGEs that formed must be from rearrangements of previous AGEs. The results showed an increase in MGH-1 formation equivalent to the decrease in MGH-DH, supporting their hypothesis. Interestingly, the results also showed that over longer periods of time, a new [M+72] AGE became the major product. Since this product could not bind to boronic acid, this AGE was determined to be CEA, which was then hypothesized to form from hydrolysis of the amide bond of MGH-1 (Fig. 2).

Gaps in Glycation Knowledge

Due to the nonenzymatic nature of glycation, as well as the variety in products that it forms, most of the chemistry behind the process is unknown. Therefore, the chemical knowledge uncovered by McEwen *et al.* has already led to numerous useful discoveries for the lab and field of glycation. For example, the understanding that AGEs can form through rearrangements has

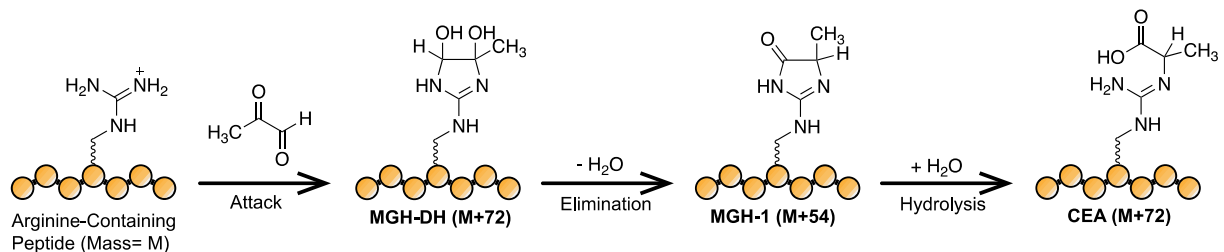


Figure 2. Proposed Mechanistic Connection Between AGEs. Experiments from McEwen *et al.* in the Scheck Lab support their proposed mechanistic connection between MGH-DH, MGH-1 and CEA.¹³ After attack on the carbonyl groups of MGO by arginine, MGH-DH is formed. Then, through the abstraction of a hydrogen and loss of a hydroxide group, followed by tautomerization, MGH-1 is formed next. Finally, hydrolysis of the amide bond of MGH-1 forms CEA. It is important to note that both MGH-DH have the same mass of M+72, but appear at different stages of the reaction.

sparked new hypotheses of the mechanisms of other AGEs, such as APY. Additionally, knowing the importance of the elimination step in forming MGH-1 has allowed the group to synthesize arginine-containing peptides with sequences that promote the formation of these AGEs by putting a general base, tyrosine, close enough to participate in the elimination step of the mechanism. Not only does this provide a helpful model to study glycation, but it has led to studies of the effects of amino acid sequence on the glycation of proteins, as well as the promotion of other AGEs. This exemplifies how vital uncovering almost any chemistry involving glycation can be, as it leads to both more effective tools for future research and new concepts to explore.

With such chemical knowledge of the numerous other AGEs formed from MGO, more potential connections can be uncovered. This gap in knowledge is problematic as glycation has been linked to a variety of different diseases, such as diabetes, Alzheimer's, and cancer.¹²⁻¹⁴ Without a better chemical understanding of the process, connections between different AGEs and disease will continue to remain unknown. Additionally, therapeutics can be made much more effective when specific mechanistic steps can be targeted, allowing potential drugs to be specialized to target a specific interaction. However, there is lack of tools available to study this process, as traditional tools for studying post-translational modification often rely on the enzymatic nature of such reactions. While some specialized tools can be helpful in differentiating AGEs, they are often very limited to unique chemical features of that AGE, such as the boronic acid assay used in McEwen *et al.*, which reacts specifically with the diol of MGH-DH. Therefore, a chemical tool to study many AGEs at once is of great importance to the field of glycation.

Experimental Design

One highly appealing strategy for uncovering connections between AGEs, applicable to every AGE formed by MGO, would be to isotopically label specific atoms of MGO itself. These labels are perfectly suited for MS analysis, a highly-used method for the observation of AGEs on peptides and proteins. The presence of an isotopically labelled atom could easily be observed,

as the mass of the AGE would shift one extra unit per labelled atom still attached AGE. This way, losses in specific atoms could be tracked from one AGE to the next, and mechanistic connections between AGEs could easily be drawn once the exact atoms that are leaving are known. Potential deuteration of MGO was prioritized, as many AGEs retain all three of the original carbons from MGO, making carbon labelling ineffectual. However, the hydrogens of MGO are in constant exchange as different AGEs are formed, a prime example of which being the elimination between MGH-DH and MGH-1 (Fig. 2). In this step, the original aldehydic proton of MGO is lost, which if deuterated, should then correspond to the loss of the label. Additionally, the effects of deuteration on the rates of reactions are very well understood, allowing for kinetic isotope experiments to be performed. These experiments could then glean information on the hybridization of the carbons of MGO, providing a better understanding of the mechanism. For this reason, a procedure for the synthesis of deuterated methylglyoxal was prioritized. In particular, a synthesis that could lead to deuteration of MGO at each of its unique hydrogens was prioritized, so the exact position of the loss of the label would be known.

Difficulties in MGO Synthesis

Though this small molecule has been well-studied in glycation, synthetic attempts at producing MGO face multiple difficulties due to the frustrating properties of the compound. MGO is soluble in almost all organic and aqueous solvents, ranging from benzene to water, which eliminates extraction as a viable separation method. MGO also forms multiple different structures when dissolved in water due to hydration at its carbonyl groups, whose structures must be accounted for in analysis methods such as in NMR.¹⁵ Currently, the simplest procedure for the synthesis of MGO makes use of its acetal form of its aldehyde group (methylglyoxal 1,1-dimethyl acetal), which is hydrolyzed under acidic conditions.¹⁶ However, most recent studies use commercial sources of MGO to bypass synthesizing this frustrating compound.

Synthesis Strategies

There are two unique positions for deuteration on MGO: the methyl position and the aldehyde position. Luckily, accessing the methyl position of MGO for deuteration is simple through the tautomerization between the keto and enol form of MGO (Fig. 3). Using acid to catalyze this tautomerization allows MGO to be in constant exchange with protons in the solvent. Using D-Cl and D₂O, complete incorporation of deuterium into only the methyl group of MGO was observed, forming d₃-MGO.¹⁷ This tautomerization can be catalyzed under acidic or basic condition, but acid was favored due to potential base-catalyzed reactions of the MGO enolate.

However, deuteration of the aldehydic position of MGO is much more challenging, as no such quick chemistry exists for simple deuterium exchange. For this position, synthesis of MGO from a deuterated precursor would be required. Though the previously mentioned methylglyoxal 1,1-dimethyl acetal precursor was briefly considered, the aldehydic position of the acetal is just as difficult to access, so other synthetic strategies were sought out. After a review of the literature,

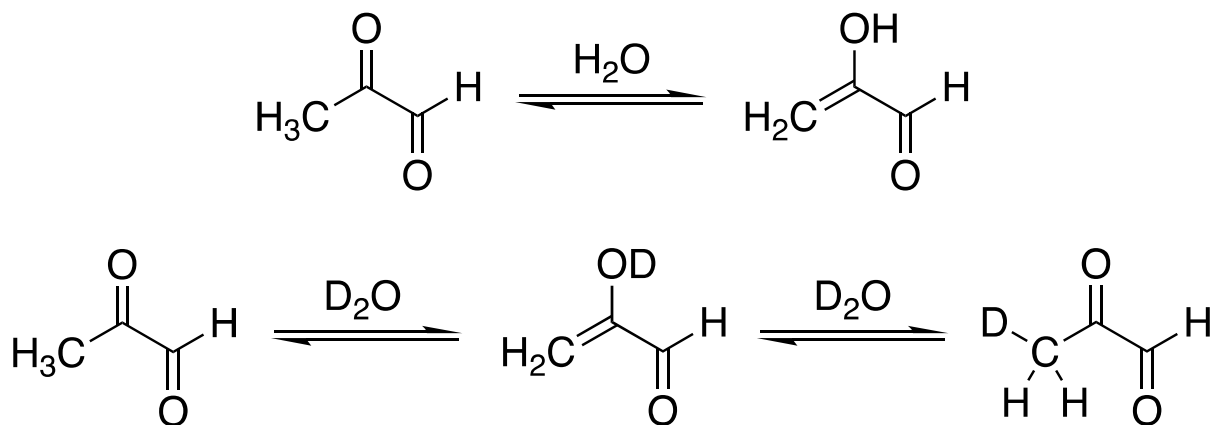


Figure 3. Tautomerization of MGO in Water and D₂O. Above: Through the interaction of MGO and two water molecules, one carbonyl of MGO is protonated, while a methyl hydrogen is abstracted, forming the enol. Below: In D₂O, this tautomerization leads to the replacement of a methyl hydrogen with a deuterium label. This process then repeats for the other methyl hydrogens, until the methyl group is completely deuterated.

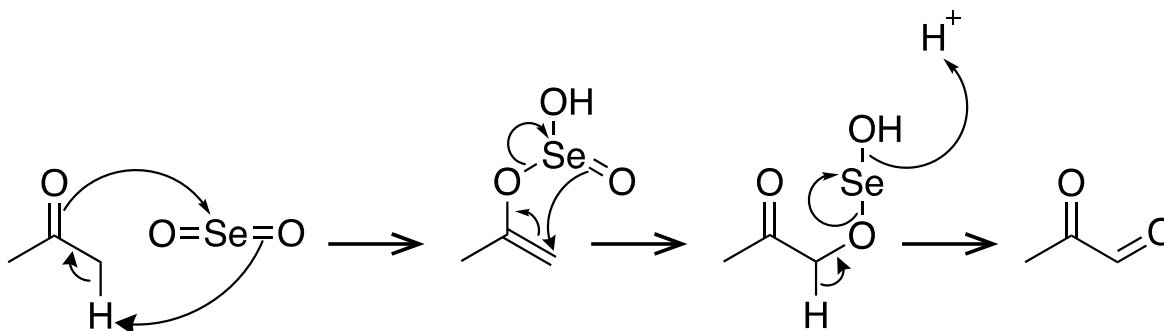


Figure 4. Proposed Mechanism of Riley Oxidation. This pericyclic mechanism was proposed by Shah *et al.* Acetone and selenium dioxide react to form MGO, forming selenium and H_2O as by-products.

the Riley Oxidation¹⁸, which uses selenium dioxide to form MGO from acetone, was identified as the optimal choice (Fig. 4).¹⁹

Acetone is not only an ideal starting material, but deuterated acetone is also commercially available in high purity as an NMR solvent. This also removes the potential loss in yield and purity in the deuteration of the starting material, saving time and increasing overall yield. Using Riley Oxidation in combination with the tautomerization reaction of MGO, it is now possible to form fully deuterated MGO (d4-MGO) from fully deuterated acetone, and then to remove the deuterium labeling at the methyl group using H-Cl in H_2O to form aldehydically labelled MGO (d1-MGO) (Fig. 5), as the aldehyde group was confirmed to be unaffected by the tautomerization reaction done by Königstein *et al.*¹⁷ In summary, these two synthesis protocols give relatively easy access non-

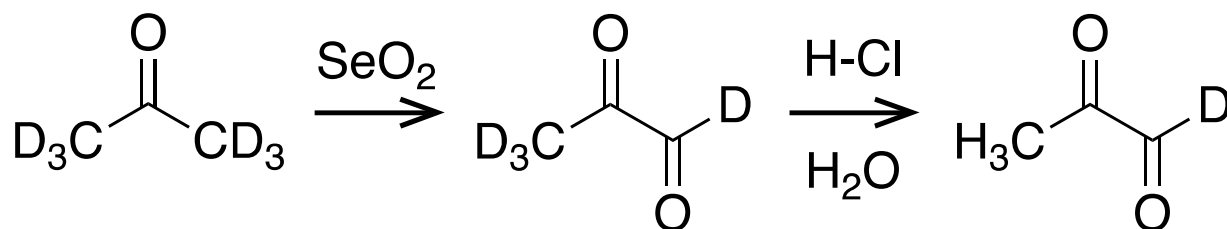


Figure 5. Isotopic Labelling of the Aldehyde Group of MGO. Beginning with deuterated acetone, Riley Oxidation forms fully deuterated MGO. Once this fully deuterated MGO is synthesized, it can then be subject to hydrogen/deuterium exchange in acidic conditions, promoting the tautomerization of the MGO and loss of the methyl deuterium atoms.

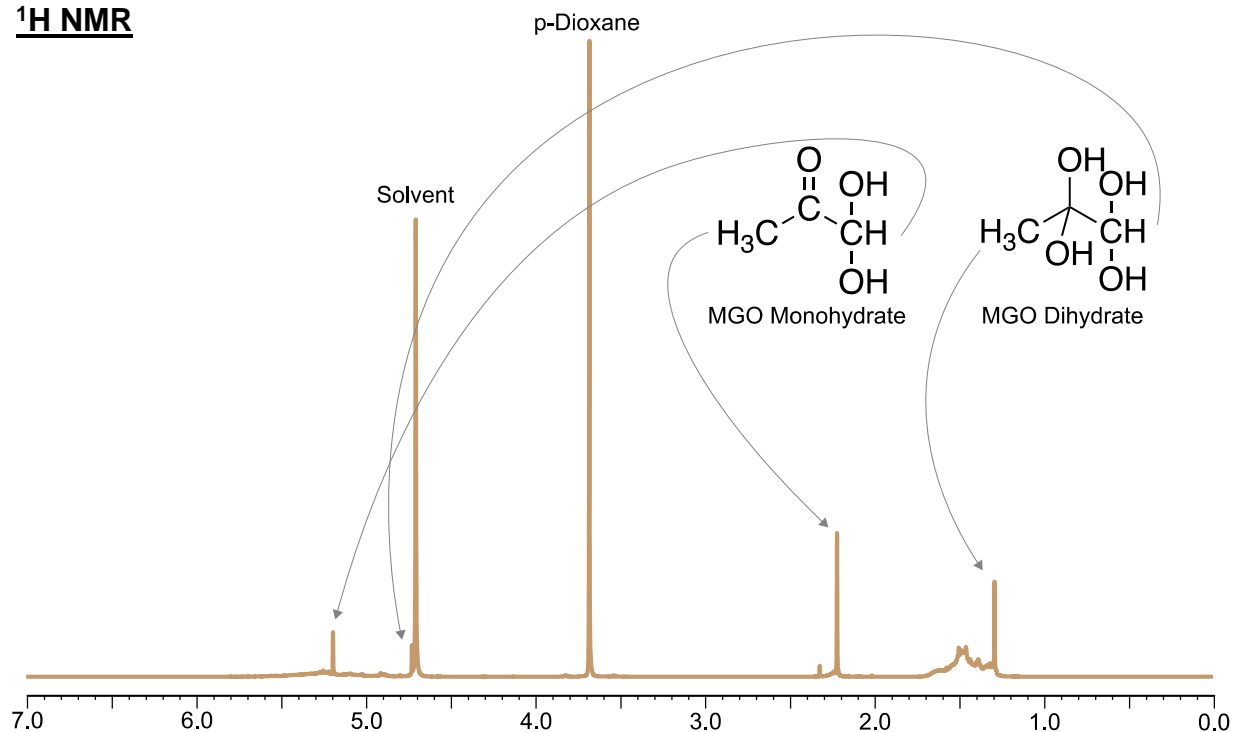
deuterated MGO, as well as d1-MGO, d3-MGO, and d4-MGO, for use in analyzing the AGEs formed from glycation reactions using these deuterated forms of MGO.

4. Results

Preliminary Riley Oxidation Results

First, the effectiveness of the Riley Oxidation procedure was tested. Upon ^1H NMR analysis of the final products, singlet peaks corresponding to monohydrate MGO ($\delta = 5.2$ ppm and 2.2 ppm) were instantly recognizable (Fig. 6). Integration between monohydrate aldehyde and methyl peaks was 1:3.5, only slightly above the expected 1:3, likely due to unreacted acetone with the same shift ($\delta = 2.2$ ppm). Dihydrate MGO ($\delta = 4.7$ and 1.3 ppm) was also visible, though the aldehyde peak is difficult to discern from the residual solvent peak of D_2O ($\delta = 4.7$ ppm). These values are consistent with all other studies of MGO using D_2O as a solvent, along with the multiplets ($\delta = 1.5$ ppm) corresponding to MGO polymerization.¹⁵ The last and largest peak at

^1H NMR



¹³C NMR

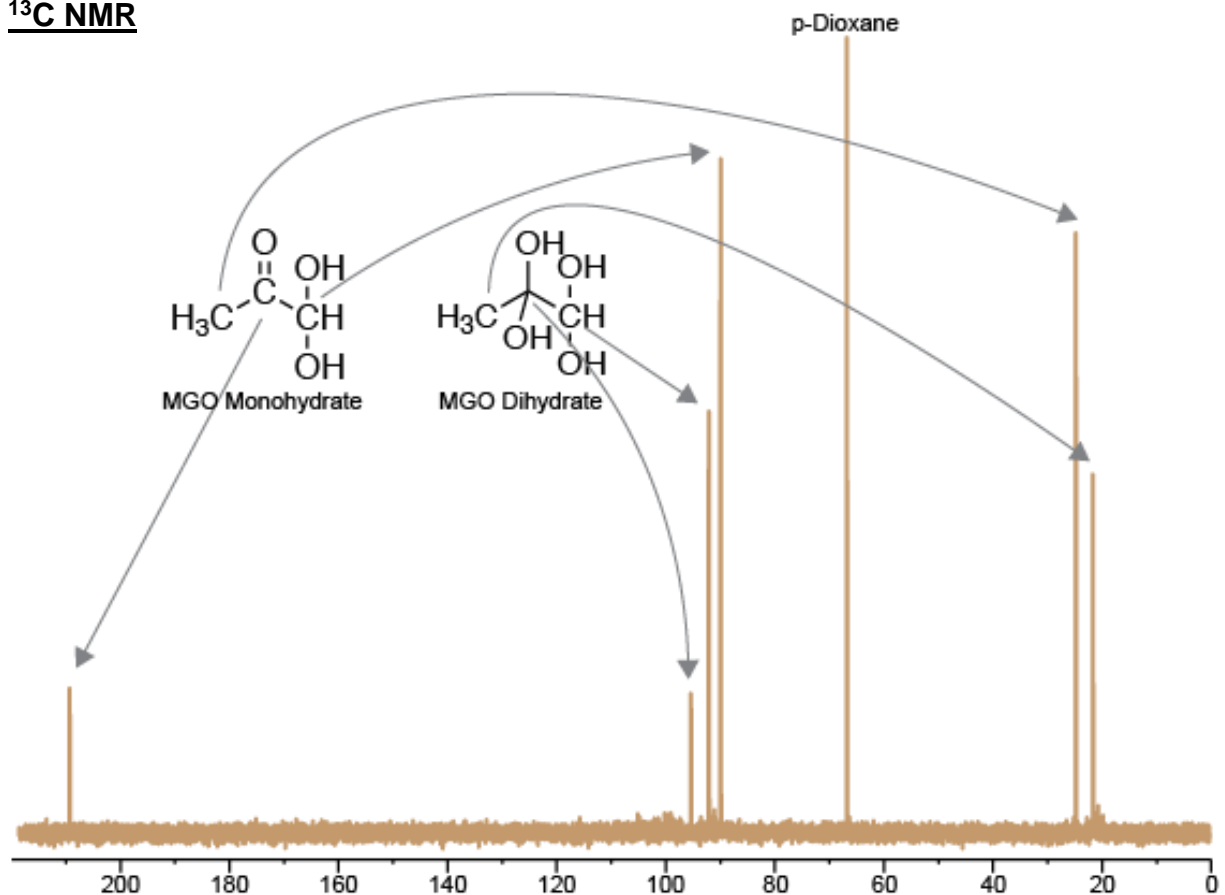


Figure 6. Initial Riley Oxidation NMR Results. A) NMR results in D₂O, in which MGO is found in its hydrated forms. Proton peaks corresponding to each hydrogen are labeled. Additional p-Dioxane peak at 3.7 ppm and MGO polymer peaks are visible centered around 1.5 ppm.¹¹ All peaks are singlets. B) Once again hydrated MGO and p-Dioxane peaks are visible. These results match the spectra of other studies of MGO in D₂O.

3.7ppm corresponds directly to p-dioxane, a solvent during the reflux of the Riley Oxidation procedure. These results were supported through ¹³C NMR analysis, in which 3 monohydrate peaks ($\delta = 209, 90$ and 25 ppm), 3 dihydrate peaks ($\delta = 95, 92, 21$ ppm), and a p-dioxane peak (67 ppm) were once again visible (Fig. 6).

Riley Oxidation without p-Dioxane

After modifying the Riley oxidation procedure to exclude p-dioxane, ¹H NMR was once again performed on the product (Fig. 7, Purple) and compared to the previous Riley Oxidation procedure (Fig. 7, Brown). The p-dioxane peak at 3.7ppm is noticeably absent, while

¹H NMR

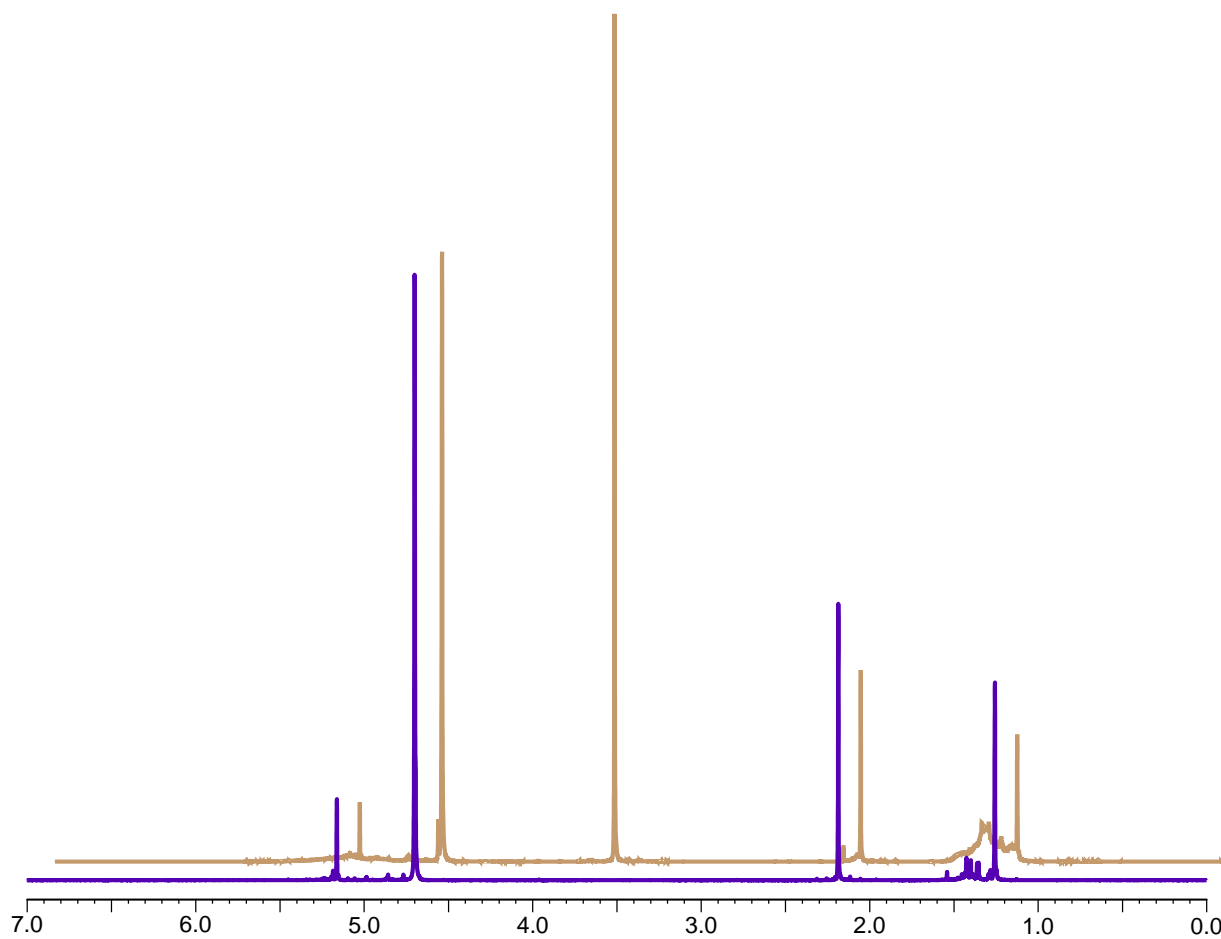


Figure 7. Comparing Riley Oxidation Procedures. In purple is the ¹H NMR of product without p-dioxane as a solvent, and in brown is the ¹H NMR from the initial Riley Oxidation procedure (Fig. 6A). Peaks were identical aside from the lack of the p-Dioxane peak at 3.7 ppm, proving the removal of the contaminant to be successful.

monohydrate and dihydrate MGO peaks were maintained. ¹³C NMR confirmed the purity of the MGO, as no other carbon peaks were observed. The synthesis yielded 20 mg of MGO, corresponding to a 6.9% yield. While not ideal, this yield is acceptable, as glycation reactions at 1 mM of MGO only use 3.6 μg of MGO per replicate. Therefore, a multitude of reactions can still be performed from one synthesis.

Glycation After 3hr, 37°C

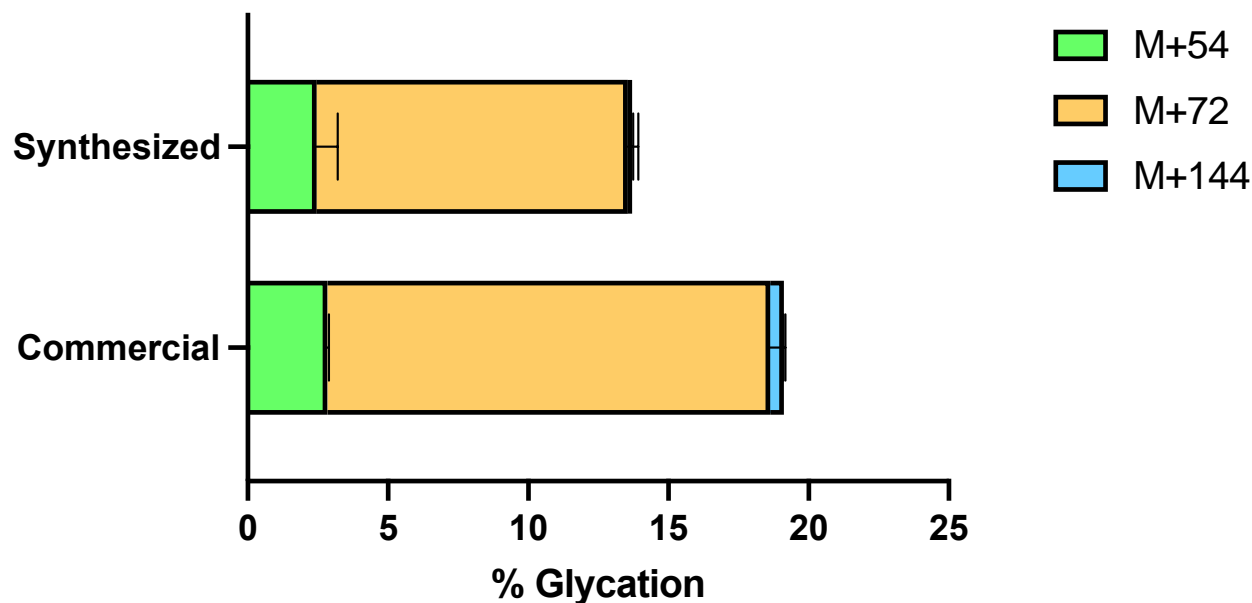


Figure 8. Glycation Results after 3hr. Synthesized MGO resulted in significantly lower total % glycation than commercial MGO.

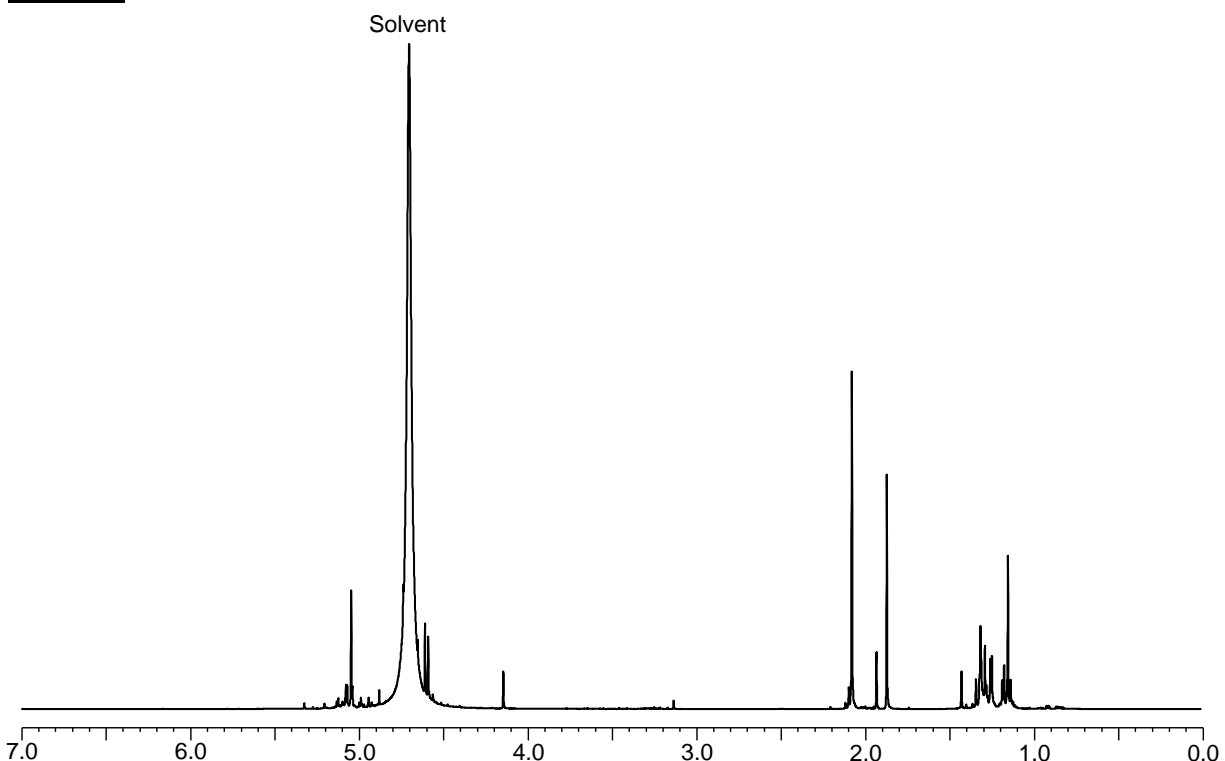
Glycation Using Synthesized MGO

To test the functionality of synthesized MGO in comparison to commercially available MGO, glycation reactions were performed on peptide (N-acetylated, sequence LESRHYA) at 1 equivalent MGO (1mM peptide and MGO). After 3 hours in 37°C, the reactions were quenched, and LCMS analysis of unmodified peptide and AGEs was performed. LCMS results were then analyzed to determine the % glycation of each peptide (Fig. 8). Synthesized MGO showed significantly lower total % glycation ($\frac{\text{Peptides with AGE adducts}}{\text{Unmodified + Modified Peptide}} \times 100$) in comparison to commercial MGO. However, it is known that glycation is highly sensitive to MGO concentration. Therefore, it is unknown whether this difference is due to the MGO itself, or a difference in actual concentrations of the MGO solutions.

Purity of Commercial MGO

In order to determine whether a difference in purity was causing the difference in the glycation of synthesized and commercial MGO, ^1H and ^{13}C NMR was taken of commercial MGO. Through this, we discovered that many new peaks are observed in the ^1H NMR of commercial MGO (Fig. 9) that do not show up in the NMR of synthetic MGO (Fig. 6). While some peaks can be attributed to monohydrate MGO ($\delta = 5.1\text{ppm}$ and 2.1ppm) and dihydrate MGO ($\delta = 1.15\text{ppm}$), peaks at 1.9ppm , 4.1ppm , and 4.6ppm are harder to understand. Additionally, the “MGO polymer” region that was small in synthetic MGO (Fig. 6) is much larger in commercial MGO, potentially signaling that a higher amount of polymerization in commercial MGO is causing this messy NMR. The ^{13}C NMR of commercial MGO is even more confusing than its ^1H NMR. Though there should only be 6 peaks total from monohydrate MGO ($\delta = 210.1, 89.7$ and 24.5 ppm), and dihydrate MGO ($\delta = 95.1, 91.9, 21.42$ ppm), many new peaks can be seen. Many of these new peaks lie in the hydrated carbon region, potentially suggesting that polymerization is occurring at these

^1H NMR



¹³C NMR

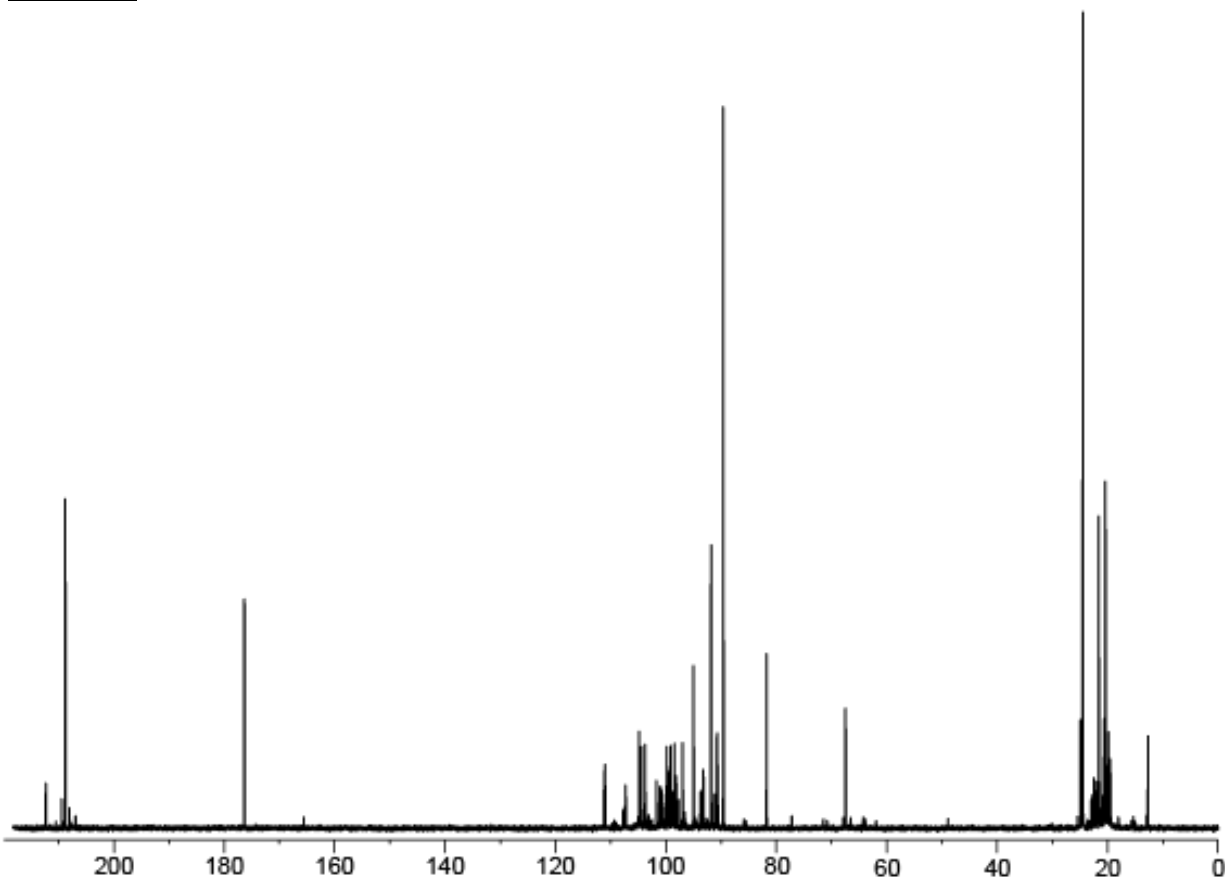


Figure 9. NMR Analysis of Commercial MGO. A multitude of new peaks show up in the NMR of commercial MGO when compared to synthetic MGO (Fig. 6), indicating that synthetic MGO is likely more pure than commercial MGO.

hydrated carbons. Such polymerized structures have also been hypothesized in the literature.¹⁵

These NMR results suggested that synthesized MGO may be more pure than commercial MGO, and purity was ruled out as a cause of the discrepancy in glycation.

Correcting Synthesized MGO Concentration

Next, the concentration of synthesized MGO was determined through a 3,4-diaminobenzophenone (DABP) assay, in order to determine whether differences in concentration were causing the difference in glycation. DABP reacts irreversibly with MGO in a Schiff base mechanism, forming a DABP-MGO complex with an extra aromatic ring. When run through analytical HPLC, unique and separate peaks from unreacted DABP and DABP-MGO complex

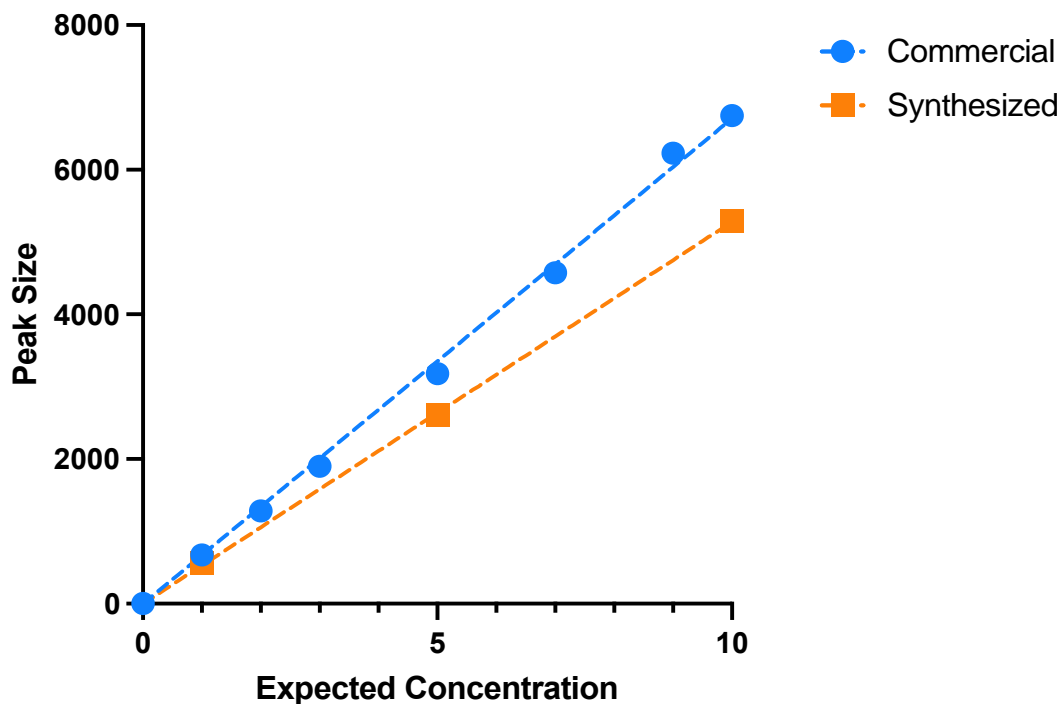


Figure 10. Comparing Actual Concentrations of MGO. DABP was allowed to react with solutions of MGO for 30 minutes at 37°C. Error bars are not visible due to being too small.

can be observed. By allowing the DABP and MGO reaction to run to completion under excess DABP, the area under the DABP-MGO peak is then proportional to the original amount of MGO in solution. Commercial and synthesized solutions of the same volume and concentration should have equivalent DABP-MGO peaks, unless one of the solutions is not of the expected concentration. Through this assay, the synthesized MGO concentration (Fig 10, orange) was found to be approximately lower than expected, using the commercial MGO (Fig. 10, blue) as reference. To determine the actual concentration of MGO in each solution, the peak size was inputted into the formula of the linear regression of the commercial MGO. The actual concentration was calculated to be on average 20% lower than expected, meaning the concentration of synthetic MGO in the glycation reactions was actually at 0.8 mM instead of the usual 1 mM.

Glycation After Concentration Correction

Glycation After 3hr, 37°C

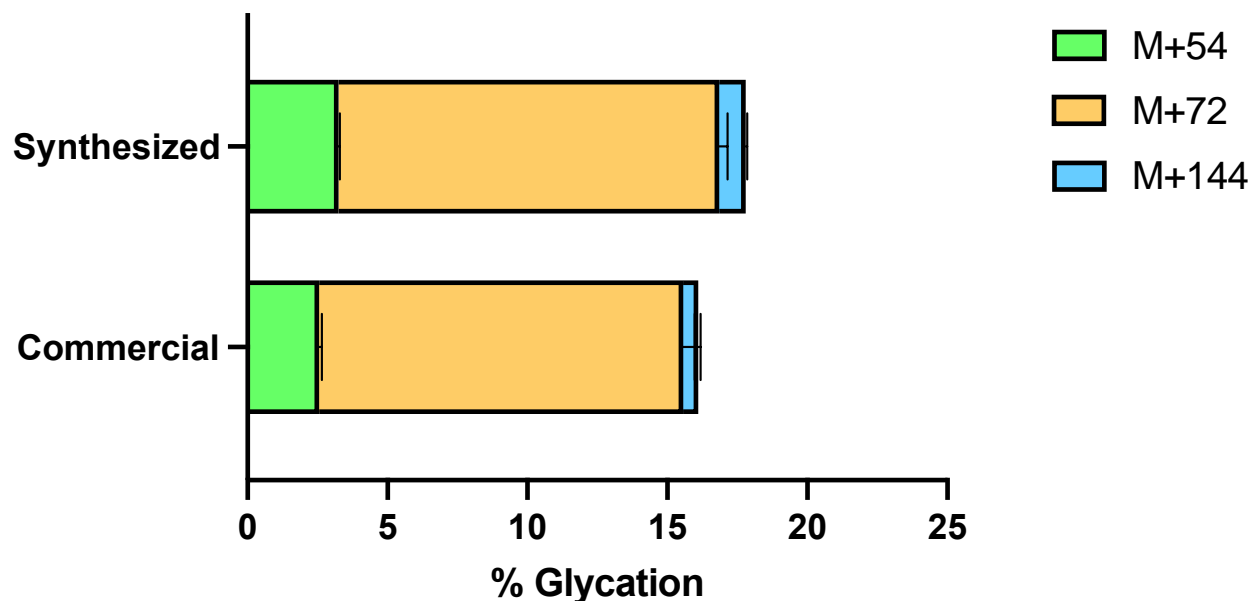


Figure 11. Glycation after Corrected Concentration. After correction of synthesized MGO concentration, glycation was once again compared between synthesized and commercial MGO. Synthesized MGO outperformed commercial MGO in terms of total % glycation, and formed more of each individual AGE as well.

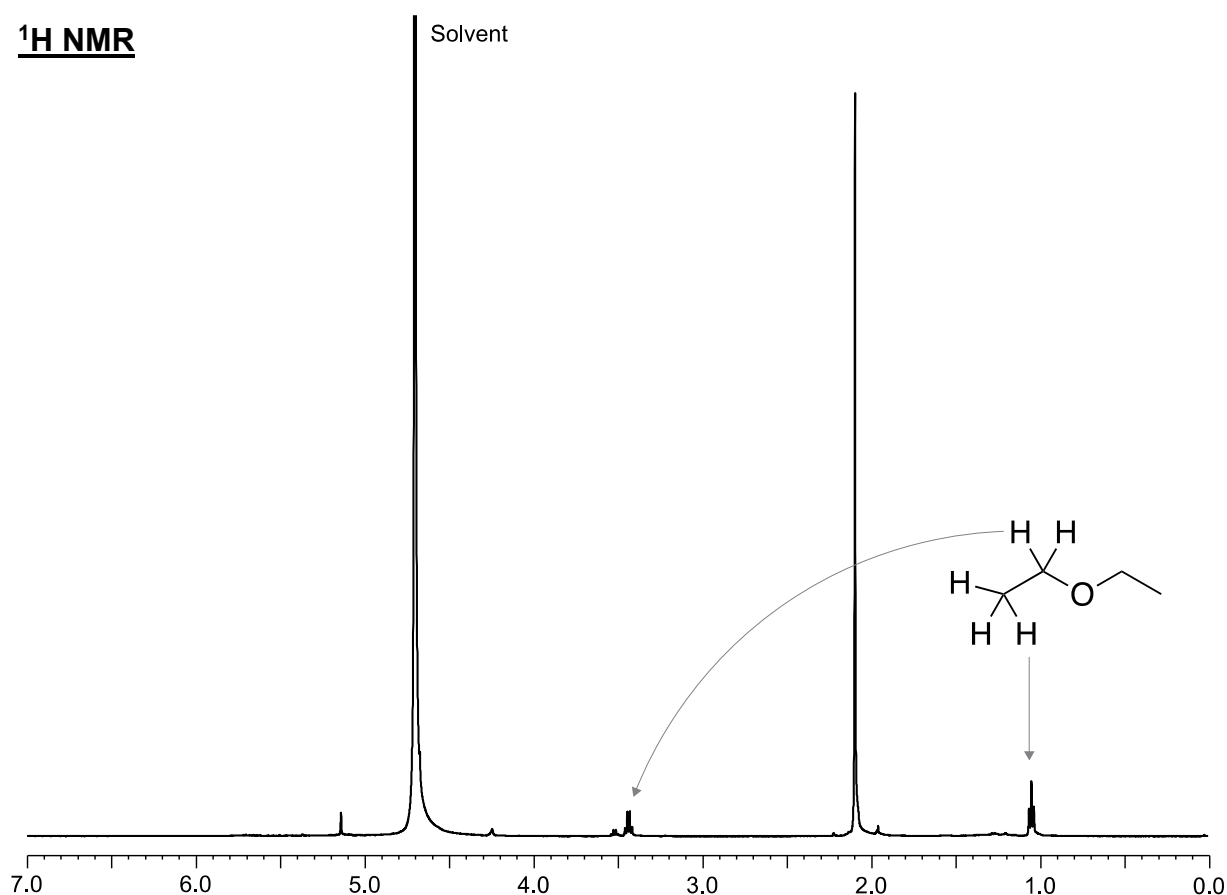
Glycation experiments were once again performed, using the corrected concentration value for the synthesized MGO. In this experiment, synthesized MGO had significantly higher percent glycation after 3 hours (Fig. 11). This increase could be attributed to the synthesized MGO being newer than the commercial MGO, meaning less polymerization between MGO molecules, and more MGO available to participate in glycation. These experiments proved that the lower original glycation values were due to errors in concentration, and that synthesized MGO is just as effective, if not more effective, as commercial MGO. From this data, Riley Oxidation was confirmed to be an adequate method for future MGO and D-MGO synthesis.

Tautomerization Reaction with Purification

In the hydrogen exchange reaction that makes use of the enolization of MGO, the reaction occurs under highly acidic conditions to promote the formation of the enol and facilitate the

addition of the deuterium labels. This strong acid had to be neutralized, leaving a high concentration of salt in the flask. Due to the solubility of MGO in both organic and aqueous solvents, salt was first attempted to be removed through distillation. However, distillation led to very low yields, often resulting in no product after water was removed through lyophilization. Though higher amounts of starting material could alleviate this issue, this would not be possible with the limited yield of the Riley Oxidation, making this purification method not applicable to d1-MGO synthesis. This prompted a revised purification strategy to remove the salt, which aimed to take advantage of the solubility of MGO in both organic and aqueous solvents. First, the neutralized product was lyophilized, leaving only salt and MGO. Next, these salt crystals were washed filtered with ether, in which the MGO could dissolve and pass through the filter, while the salt could not. Finally, the ether was evaporated in a Rotovap, leaving only MGO. ^1H NMR analysis of the product from this procedure showed characteristic quartet and triplet peaks corresponding

^1H NMR



¹³C NMR

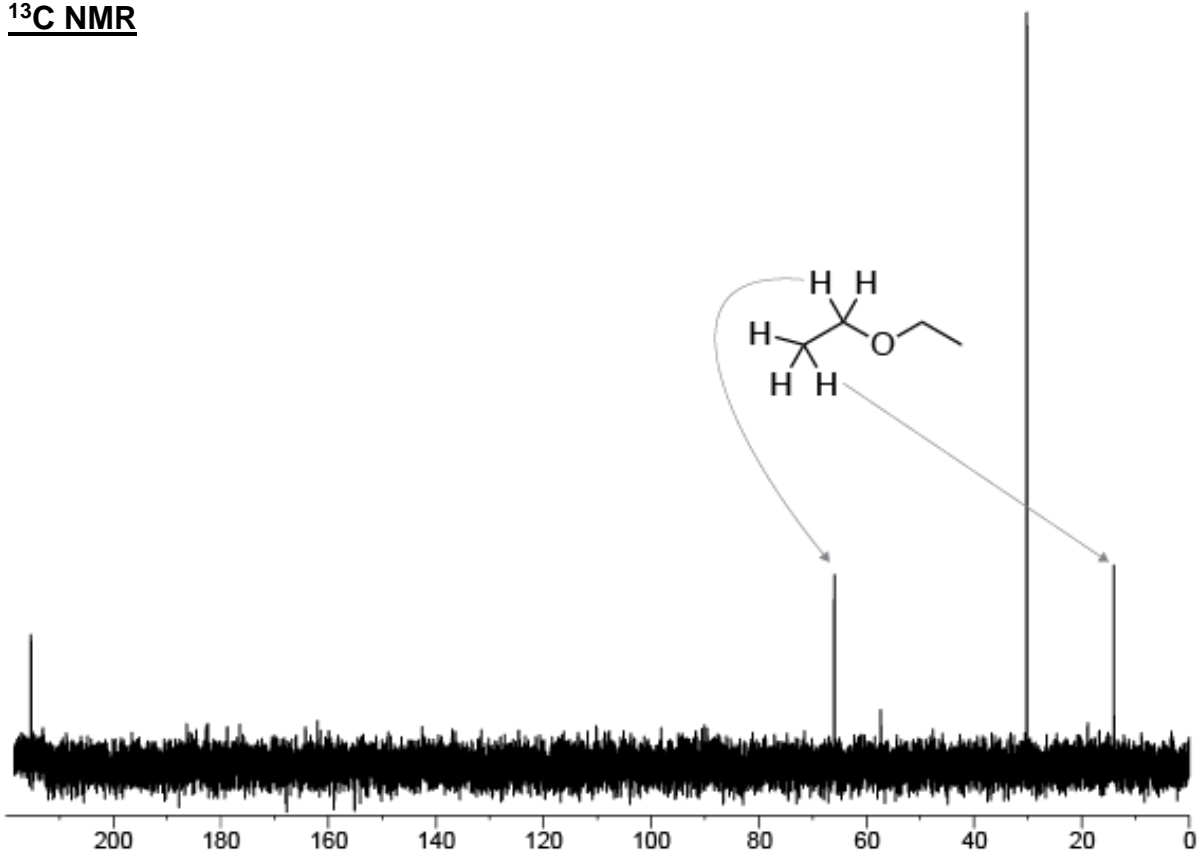


Figure 12. NMR Results after Filtration of Tautomerized Product. Arrows indicate hydrogen peaks of diethyl ether that could be identified. Solvent peak is labeled, and is partially cut off in order to make smaller peaks visible.

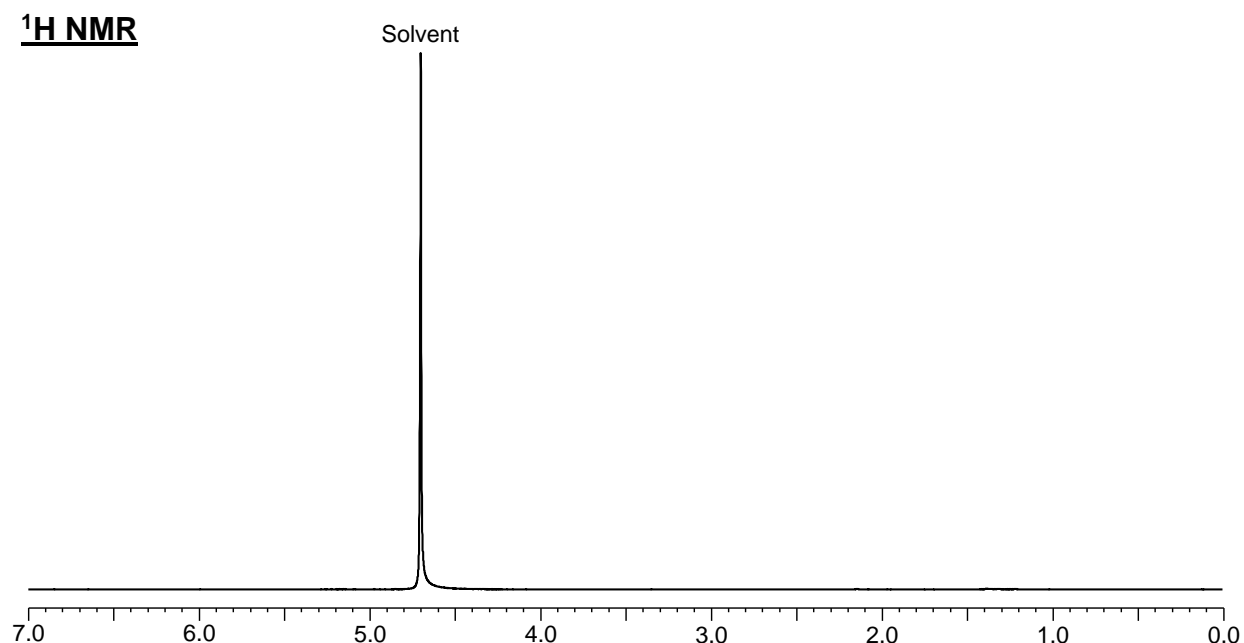
to diethyl ether ($\delta = 3.4$ ppm, quartet; 1 ppm, triplet), and other peaks that are difficult to analyze ($\delta = 5.1$ and 2.1 ppm) (Fig. 12). One possibility is that these peaks could represent undeuterated, monohydrate MGO (usually $\delta = 5.2$ and 2.2 ppm). However, the integration of the potential methyl peak ($\delta = 2.1$ ppm) was 30 times greater than that of the potential aldehyde peak ($\delta = 5.1$ ppm), completely perplexing when the methyl group should be invisible due to its deuteration. ¹³C NMR analysis also revealed a complete absence of hydrated peaks characteristic of MGO (usually ($\delta = 90$ -100 ppm range), further confirming that no MGO had been recovered in the purification process. Instead, these peaks match those of acetone ($\delta = 2.2$ ppm in ¹H NMR, $\delta = 216$ and 31 ppm in ¹³C NMR), that potentially had not been fully dried off of the NMR tube before use in the experiment.

Tautomerization Without Purification

Due to the failure of the second purification method, it became more important to determine whether the deuteration of the methyl group of MGO was successful. Therefore, the salts from neutralization were not removed in future experiments. Glycation reactions are run in 20 mM PBS buffer, and the salt remaining in the neutralized product would be negligible once the MGO was diluted to 1 mM (Appendix 1). Recent synthesis results using this protocol have yielded difficult to interpret NMR results (Appendix 2), due to the fact that commercial MGO was used as a starting material. Future experiments will make use of synthetic MGO in order to better assess MGO deuteration.

d4-MGO Synthesis

Completely deuterated MGO (d4-MGO) was synthesized using the Riley Oxidation protocol with fully deuterated acetone (d6-acetone). Upon ^1H NMR analysis, no proton peaks of MGO were visible, indicating that the MGO had been fully deuterated (Fig. 13). ^{13}C NMR analysis



¹³C NMR

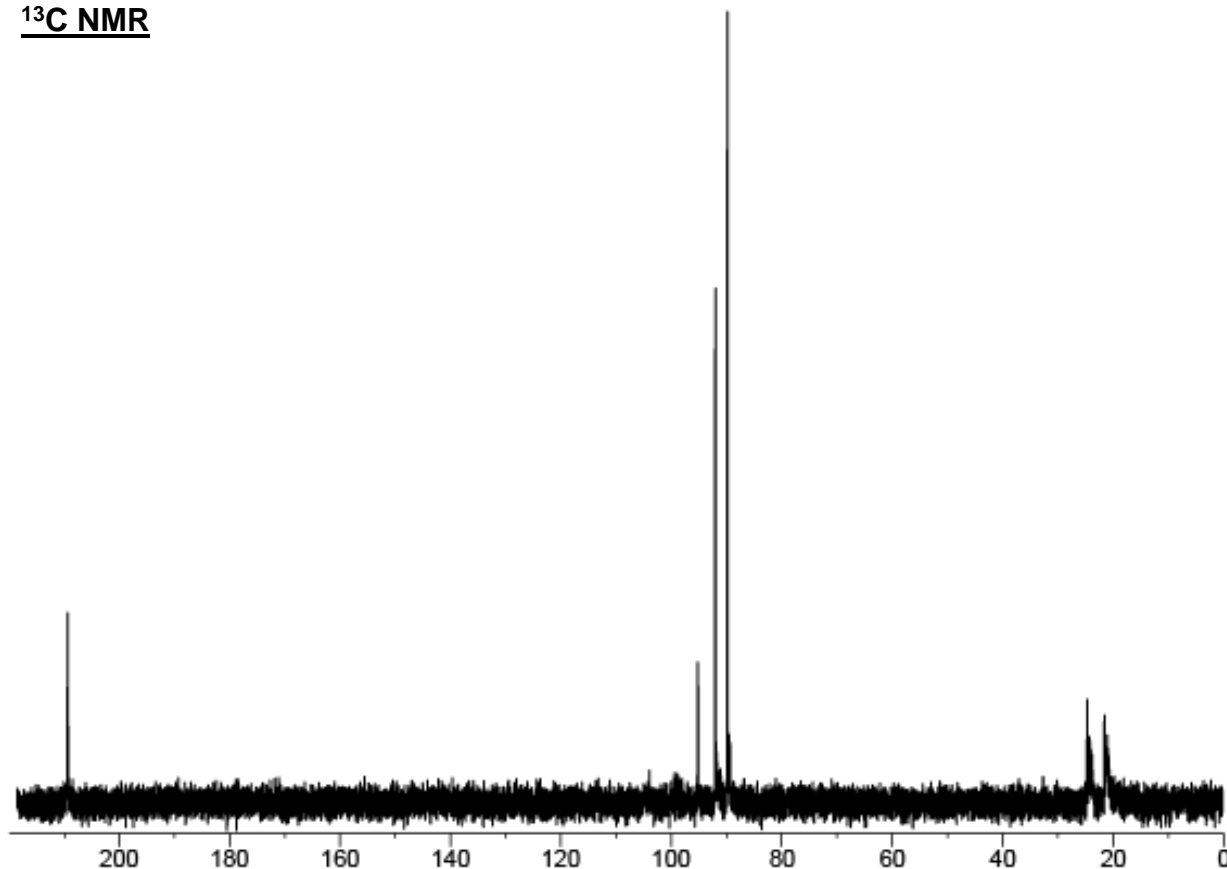


Figure 13. NMR Results of d4-MGO Synthesis. ¹H NMR results were empty, suggesting the synthesis of completely deuterated and pure MGO, or simply a lack of product. ¹³C NMR analysis showed characteristic peaks of monohydrate MGO (209, 90 and 25 ppm), and dihydrate MGO (95, 92, and 21 ppm).

showed the characteristic peaks of MGO (Fig. 13), which confirmed that the empty ¹H NMR is due to the complete deuteration of MGO, and not a complete lack of product.

Glycation Using d4-MGO

After d4-MGO synthesis had been confirmed through NMR, it was used in glycation experiments. Both commercial MGO and synthetic (but non-deuterated) MGO were run and the mass changes of AGEs were recorded 3 hours and 24 hours at 37°C after MGO was added. After 24 hours, the reactions were diluted 100x into PBS, effectively removing any free MGO from the reaction and allowing only rearrangements of AGEs to occur, as was done in McEwen *et al.* These

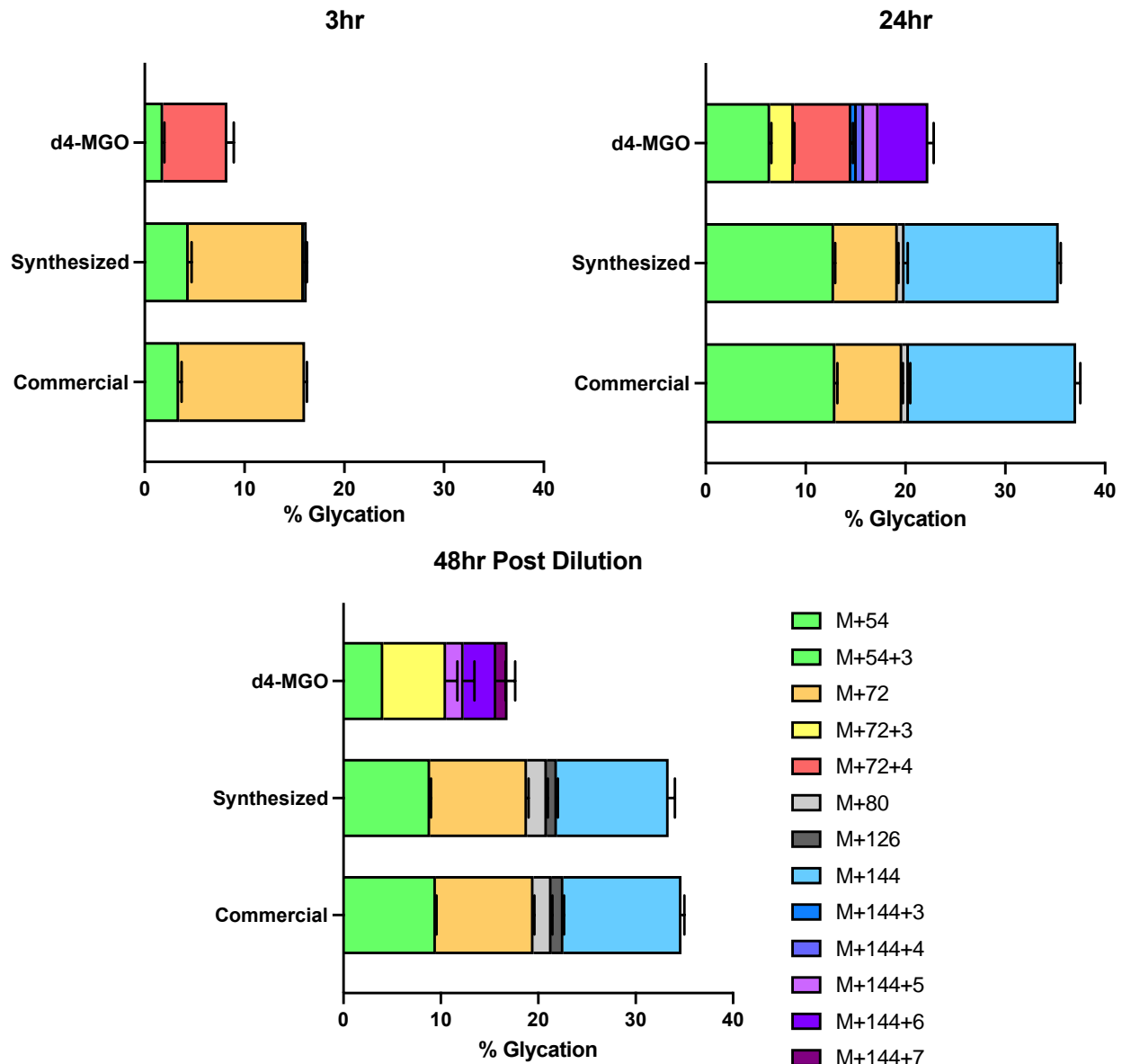


Figure 14. Glycation of d4-MGO. Glycation reactions were analyzed through LCMS after 3 hours and 24 hours, after which it was diluted to promote the rearrangement of AGEs. “Synthesized” MGO refers to non-deuterated MGO still synthesized through Riley oxidation. Different colors for M+72, M+72+3, and [M+72+4] were chosen to show how [M+72] may be a mixture of the different [M+72+3] and [M+72+4] AGEs. Similar reasoning was applied to [M+144] and its labeled counterparts.

diluted reactions were analyzed 24 hours and 48 hours after the dilution. Colors were chosen to differentiate a mixture of multiple AGEs with the same mass from individual AGEs themselves. For example, at 24 hours, the yellow CEA ([M+72+3]) and red MGH-DH ([M+72+4]) AGEs from d4-MGO are both present as isomeric [M+72] AGEs when commercial or synthesized MGO is used, thus the new orange color representing the mixture. By 3 hours, it was apparent that the

d4-MGO was glycating significantly less than both commercial and non-deuterated synthesized MGO of the same expected concentration (Fig. 14). The concentration of the d4-MGO was later analyzed for future corrections, which was found to be around 10% lower than expected (Appendix 3). Beyond a concentration correction, this difference could also be due kinetic isotope effects may be playing a role in slowing the glycation reaction down. At 3hr, d4-MGO formed only the +4 version of [M+72], at 24hr, both the +3 and +4 were visible, and at 48hr post dilution, only the +3 version of [M+72]. Additionally, labeling of [M+144] AGEs varied wildly, not only at each time point, but over the course of the experiment as well, as [M+144+7] only became visible 48hr post dilution, while [M+144+3] and [M+144+4] were only visible at 24hr.

d3-MGO, 3hr

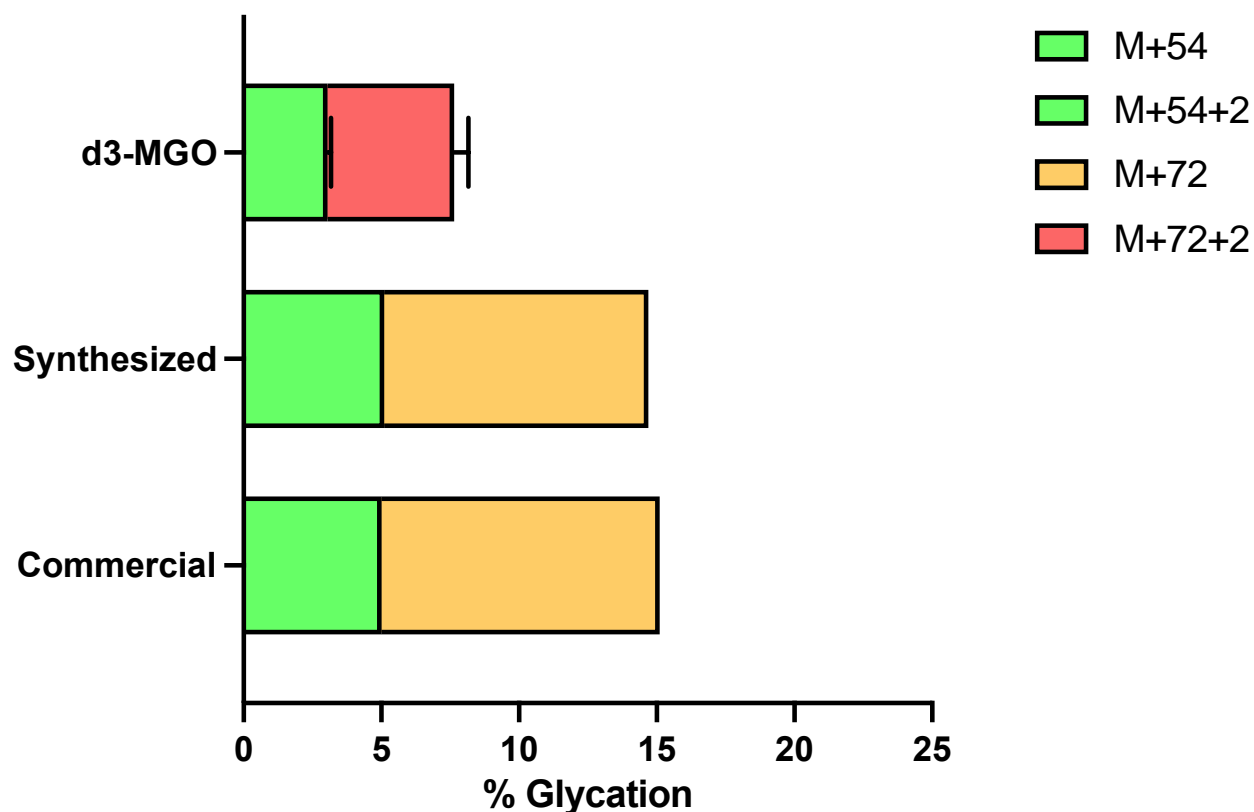


Figure 15. Glycation of d4-MGO. Glycation reactions were analyzed through LCMS after 3 hours and 24 hours, after which it was diluted to promote the rearrangement of AGEs. “Synthesized” MGO refers to non-deuterated MGO still synthesized through Riley oxidation. Different colors for [M+72], [M+72+3], and [M+72+4] were chosen to show how [M+72] may be a mixture of the different [M+72+3] and [M+72+4] AGEs. Similar reasoning was applied to [M+144] and its labeled counterparts.

Initial Glycation Results using d3-MGO

In first attempts of glycation using MGO successfully recovered from this protocol, surprising “+2” labeling was observed (Fig. 15). With our current understanding of glycation, d3-MGO should result in the +3 labeling of AGEs. Therefore, it is likely that this +2 labeling is caused by D₂-MGO, which could have been formed in the neutralization process. 5M NaOH in H₂O was used, and when pH was tested after supposed neutralization, the reaction was still highly acidic, requiring more of the base. Therefore, the introduction of hydrogens may have tampered with the complete deuteration of the methyl group of MGO. Current experiments have replaced the NaOH in H₂O with NaOD in D₂O to prevent this from happening.

5. Discussion

After a few changes to the procedure were made, Riley oxidation has been highly successful in the synthesis of both non-deuterated MGO and d4-MGO. p-Dioxane, a solvent used in Brum *et al.*, was found as a contaminant in the lyophilized product (Fig. 6), and had to be replaced with water.²⁰ More modern protocols for Riley oxidation also do not use p-dioxane, as they may have found the same difficulties regarding its contamination of the product.^{21–23} After p-dioxane was removed from the procedure, MGO appeared to be pure (Fig. 7), and was subsequently tested in glycation experiments to test whether it was as functional as standard commercial MGO (Fig. 8). Here, synthesized MGO was observed to glycate less than commercial MGO, which once again raised its purity into question. Interestingly, NMR analysis of commercial MGO revealed that commercially sourced MGO was actually less pure than synthetic MGO, likely due to its polymerization in solution (Fig. 9). The concentration of the synthetic MGO was then tested, as after lyophilization, synthetic MGO is resolubilized in a volume of water based off its weight when recorded by a scale. At the small scale of the synthesis, this scale may not be

perfectly accurate, potentially making the concentration inaccurate. Analysis through a DABP assay found that the synthetic MGO was at a concentration 20% lower than expected (Fig. 10). Once this was corrected in further glycation experiments, synthetic MGO was found to glycate slightly more than commercial MGO, likely due to its enhanced purity (Fig. 11).

This non-deuterated MGO has already become a useful tool for the field of glycation. First, it is important to know that commercial and synthetic sources of MGO are almost identical in glycation reactions. Though it has been generally accepted that the commercial sources of MGO are a suitable model for glycation, these results inform previous and future studies using commercial MGO as a glycating agent. However, synthetic MGO also maintains some helpful properties that are not shared with commercial MGO. Due to the purity of the synthesized MGO, it is easily analyzed by NMR (Fig. 6), while the NMR spectra of commercial MGO is almost impossible to recognize (Fig. 9). Other glycation projects in the lab have begun to make use of this benefit of synthesized MGO in order to perform their own NMR experiments. For example, preincubating MGO at 37°C or higher in acidic conditions leads to the increased formation of certain AGEs. Using synthesized MGO, NMR analysis of this preincubated MGO is made possible, allowing us to determine the cause of this change. Even without deuteration, synthetic MGO is has become a powerful tool that is almost necessary when doing NMR experiments on MGO, and has proven that commercial MGO is a suitable replacement for synthetic MGO in glycation experiments.

In contrast to expectations at the beginning of this project, it has turned out that the Riley oxidation protocol has been simpler to optimize than the tautomerization protocol. While Riley oxidations consistently produce MGO and d4-MGO of high enough yields, the tautomerization procedure has been fraught with revisions, without any clear results. This likely has to do with the more numerous studies that have informed our methods of the Riley Oxidation procedure.²⁰⁻²³ The tautomerization procedure was only described by a single paper, which did remove the salt from the product, leaving us with no starting point in our attempts at purification.¹⁷ This lack of

direction, combined with the already difficult properties of MGO, have added to the difficulty of this synthesis. However, after ignoring purification of the MGO, recent attempts have seemed to produce what is potentially partially deuterated MGO (Fig. 15, Appendix 2). This partial deuteration likely arose due to complications when neutralizing using a non-deuterated solvent. However, this result shows that with small adjustments, this tautomerization reaction will soon be perfected for the synthesis of d3-MGO and d1-MGO.

Using d4-MGO, hydrogens originating on MGO can be differentiated from those originating from water, which becomes incredibly useful when looking at the connection between MGH-DH, MGH-1, and CEA (Fig. 2). When using non-deuterated MGO, both MGH-DH and CEA have identical mass changes at $[M+72]$, and cannot be distinguished. Using d4-MGO reveals that two different labeled forms of $[M+72]$ appear, those being $[M+72+3]$ and $[M+72+4]$. In McEwen *et al.*, MGH-DH is proposed to be formed directly from the attack of the arginine amides to the carbonyls of MGO (Fig 2.). As no MGO protons would have yet been lost, this should result in a $[M+72+4]$ mass shift corresponding to MGH-DH. Next, the formation of MGH-1 is proposed to occur through the loss of proton and hydroxyl group of MGH-DH. This would result in the removal of one deuterium label of d4-MGO, giving MGH-1 a mass shift of $M+54+3$. Finally, CEA is proposed to form through the hydrolysis of the amide bond of MGH-1, expected to have a mass shift of $[M+72+3]$ when using d4-MGO. Glycation results using d4-MGO tell the exact same story. At 3 hours, only $[M+72+4]$ and $[M+54+3]$ are visible (Fig. 14, 3hr), correlating perfectly to MGH-DH and MGH-1, the first two steps in the pathway. As time passes, $[M+72+3]$ becomes visible at 24 hours (Fig. 14, 24hr), corresponding to CEA forming from MGH-1, the last AGE in the mechanistic pathway. Finally, 48 hours after dilution, no more $[M+72+4]$ is visible (Fig. 14), as no more MGH-DH can be formed through interactions with MGO, and MGH-DH is slowly lost as it becomes MGH-1 and CEA. This data supports this proposed connection between AGEs, providing a novel method to distinguish between AGEs of the same mass shift.

This data has also begun to raise interesting questions about the different potential structures of AGEs with mass shifts of [M+144]. The only currently known AGE structure of mass [M+144], though retention time data suggests that there are others. Interestingly, a wide variety of different mass changes were found when using d4-MGO, ranging from [M+144+3] to [M+144+7]. Though there is no clear pattern to this labeling yet, with more experiments and selectively deuterated d3-MGO and d1-MGO, the origin of these labels will become much more clear, and soon, new mechanistic connections may be formed.

The same can be said for other AGEs whose mass shifts have been observed, but for which we still lack structures or mechanistic information. One example of this is with [M+80], known as Argpyrimidine (APY) (Fig. 1). This AGE is currently being studied in other projects in the Scheck lab, due to its autofluorescent properties. The currently accepted mechanism for APY formation, however, has many issues that have not yet been addressed. It has been proposed that to form APY, two MGO molecules rearrange to form a reductone structure, which then attaches to arginine, eventually forming APY (Fig. 16).²⁴ The most questionable mechanistic step for this reaction occurs when one MGO molecule attacks another through the formation of an acyl carbanion, a very high energy intermediate, forming a reductone. However, the authors proposing this step do not directly show that MGO can form this reductone molecule, instead opting to directly add a reductone precursor to arginine, from which APY was formed. The authors support this with the explanation that the reductone likely is too short-lived to be observed. Though this does show that the reductone can form APY, it does not directly show that MGO forms APY

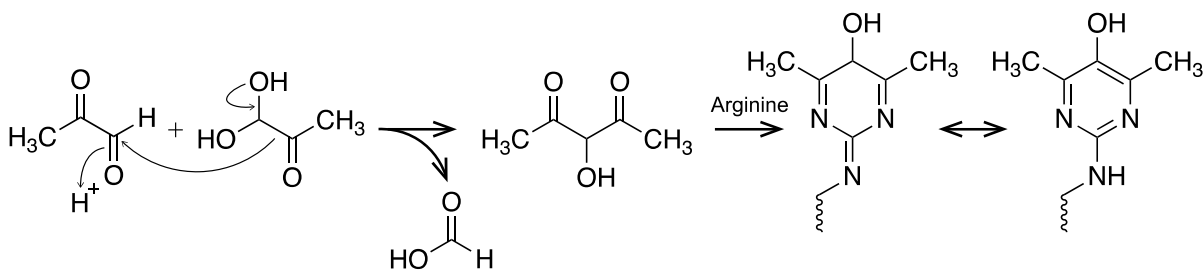


Figure 16. Currently Accepted APY Mechanism. The authors did not prove the formation of the reductone intermediate.

through this mechanism, something deuterated MGO can confirm or deny. Previous work has also uncovered a potential connection between the decrease in [M+144] and the increase in APY, suggesting a mechanism may connect the two.¹¹ With a better understanding of the origins of hydrogens on both [M+144] and [M+80], this potential mechanistic connection can be examined even deeper.

Though using deuterated MGO in glycation experiments has yielded novel results, certain limitations have to be addressed. The presence of deuterium labeling supports the previously proposed mechanism, but does not prove its existence, as deuterium labeling is not a structural technique. Additionally, the current data cannot yet distinguish between which deuterium is being lost when comparing MGH-DH to MGH-1 and CEA, as the d4-MGO is labeled at both the methyl and aldehydic position. However, future glycation using d1-MGO and d3-MGO will allow such distinctions to be made. Though there is still much confusion in regard to the chemistry of glycation, deuterated MGO has incredible potential uncover even more about the process than what has been described here.

6. Conclusion

Pure MGO, just as functional as commercial sources, has been successfully synthesized from acetone through Riley Oxidation. By making use of this reaction and the tautomerization of MGO, it will soon be possible to produce both d3-MGO and d1-MGO. In the meantime, synthesized MGO has had numerous benefits in aiding to understand the chemical machinations of glycation. Synthesized MGO itself is highly useful for NMR analysis of MGO and the structures it may form. Additionally, d4-MGO formed from Riley Oxidation of deuterated acetone has is able to differentiate many AGEs that would normally of the same mass, such as MGH-DH and CEA. Using d4-MGO, MGH-DH is labeled as M+72+4, while CEA is labeled as M+72+3, allowing for analysis of the AGEs specifically. Additionally, these results suggest that there are many different

structures of AGEs with mass [M+144] , aside from the known structure of THP. These results also directly support the mechanistic connection between MGH-DH, MGH-1, and CEA proposed by McEwen *et al.* Future work will begin to inform the field of glycation on the mechanisms behind AGEs such as THP and APY, while potentially giving information as to new AGE structures. Deuterated MGO has already had a massive impact on our chemical understanding of glycation, and is leading the way toward a complete understanding of the network between AGEs in the body.

7. Methods

General NMR Procedure

D₂O (99 atom % D, MilliporeSigma) was used as NMR solvent for analysis in a Bruker Avance III 500 MHz NMR. Chemical shifts of ¹H NMR were determined using D₂O (4.79 ppm) as a reference. ¹H NMR were run using 16 scans at 1 s relaxation delay. ¹³C NMR were run using 800+ scans at 2 s relaxation delay.

Riley Oxidation Procedure – With p-Dioxane

Reactants were added in proportions according to Brum *et al.* at a scale of 4 mmol acetone and SeO₂ (MilliporeSigma) and 28 mmol p-Dioxane (MilliporeSigma).²⁰ After reflux with stir bar on an oil bath at 100°C for 4 hours, the flask was attached to a short path distillation head and distilled on an oil bath at internal temperatures and fractions according to Brum *et al.*²⁰ leaving pale yellow distillate in the fractions. All fractions were then lyophilized in a Labconco -105°C lyophilizer overnight, leaving a taffy-like yellow substance.

Riley Oxidation Procedure – Without p-Dioxane

10 mmol acetone and SeO_2 were added to roughly 5 mL H_2O in a round bottom flask with stir bar for reflux on an oil bath at 100°C for 4 hours. After this time, the flask was attached to short path distillation head and distilled into one fraction at internal temperature of 100°C . The pale yellow distillate was then lyophilized overnight, leaving the taffy-like yellow MGO product.

Tautomerization Method – With Distillation

1 mmol of MGO (40% w/v in water, MilliporeSigma) was added to a 5 mL solution of 3M DCI (35% w/v in D_2O , MilliporeSigma) in D_2O (99 atom % D, MilliporeSigma) with stir bar, capped with a septa and put under argon, and heated at 50°C overnight. Reaction was then cooled in ice and neutralized using 1.41 mL (15 mmol) of 5M NaOH. Neutralized reaction was then attached to short path distillation head and distilled at 100°C internal temperature using an oil bath. Product was then lyophilized and resolubilized in D_2O for NMR analysis.

Tautomerization Method – Filtration and Evaporation

8 mmol of MGO were added to a 5 mL solution of 3 M DCI in D_2O with stir bar, capped with a septa and put under argon, and heated at 50°C overnight. Reaction was then cooled in ice and neutralized using 1.4 mL (15 mmol) of 5 M NaOH, after which it was lyophilized overnight, leaving browned salt crystals. These crystals were washed with diethyl ether ($\geq 99.8\%$, MilliporeSigma) and allowed to filter through (Whatman) until crystals lost brown color. The yellow flowthrough was collected and evaporated in a Heidolph Rotovap for a couple of minutes, until liquid was evaporated.

Tautomerization Method – No Purification

8 mmol of MGO were added to a 5 mL solution of 3M DCI in D_2O with stir bar, capped with a septa and put under argon, and heated at 50°C overnight. Reaction was then cooled in ice and neutralized using 40% w/v of NaOD in D_2O (40% w/v in D_2O , MilliporeSigma).

Peptide Synthesis and Purification

Peptide was synthesized by Colby Girard, another undergraduate in the Scheck Lab. 200mg of Ala-Wang resin was used for solid-phase peptide synthesis in a 6 mL fritted syringe. Washes were done with dimethylformaldehyde (DMF), and 20% piperidine in DMF was used for deprotection of Fmoc groups. 5 equivalents of Fmoc-protected amino acids (ChemPep and Advanced ChemTech) were added to 5 equivalents of O-(benzotriazol-1-yl)-*N,N,N',N'*-tetramethyluronium hexafluorophosphate (193.4 mg HBTU, Alfa Aesar) and 10 equivalents of *N,N*-diisopropylethylamine (177.7 μ L DIPEA, TCI Chemicals) for coupling. Peptides were then acetylated at the N-terminus using 4 equivalents acetic anhydride and 3 equivalents DIPEA in 2 mL of DMF for 2 hours. Resin was then washed in the syringe with dichloromethane (DCM) and dried in a desiccator overnight. Peptide was then cleaved from the resin using 95% trifluoroacetic acid (TFA), 2.5% triisopropylsilane, and 2.5% water in a total volume of 8mL for 2 hours, and then dried under air overnight. For purification, dried peptide was solubilized in a 50/50 mixture of acetonitrile and water. This was then purified through high-pressure liquid chromatography (HPLC) using an Agilent 1260 LC system equipped with an Agilent ZORBAX SB-C18 column (9.4 \times 250 mm²), 5 μ m particle size employing water and acetonitrile mobile phase with 0.1% TFA. Absorbance at 215 and 280 nm was used to observe desired peptide peaks, which were then collected using an automated fraction collector. Pure fractions were then lyophilized before stock peptide solution was prepared at 20 mM in DMF.

Glycation Procedure

Replicates for glycation were set up in microcentrifuge tubes. Each tube contained 32.5 μ L Milli-Q water, 10 μ L phosphate buffered saline (PBS) from a 100 mM PBS stock at pH of 7.3, 2.5 μ L peptide from a 20 mM stock of N-acetylated peptide of sequence LESRHYA in a 1:1 DMF/water solution, and 5 μ L of MGO (either synthesized or from MilliporeSigma at 40% w/v in

water) from a 10 mM stock solution in water. This results in samples of 50 μL total volume containing 20 mM PBS, 1 mM peptide and 1 mM MGO. Microcentrifuge tubes were then capped, spun, heated in a 37 °C water bath for at least 3 hours. Some reactions were diluted by 100x after 24 hours, placing 10 μL of the reaction into 990 μL of 20 mM PBS. For LCMS analysis, 3 μL of reaction was quenched in 300 μL water and 3 μL of 500mM Tris.

LCMS and Data Analysis

Reversed-phase liquid chromatography and mass spectrometry (LCMS) analysis was done using an Agilent 1260 Infinity LC system inline with an Agilent 6530 Accurate Mass Q-TOF. Replicates were injected onto an AdvanceBio Peptide 2.7 μm column (2.1 x 150 mm, Agilent). Analysis of MS data was done using Agilent MassHunter BioConfirm Qualitative Analysis software and PEAKS Studio (v. 7.5) software. MS data was quantified using the MassHunter Molecular Feature Extractor, which reports cumulative MS ion counts as 'volumes' observed for any and all charge states associated with a particular ion. Percent glycation of each AGE was found by dividing the volume of that AGE by the sum of all glycated and unmodified peptide. Error bars were determined using SEM.

Diaminobenzophenone (DABP) Assay

Samples ranging from 0 to 10 mM MGO with 25 μL total volume were formed in high-recovery vials (Agilent) from different amounts (0-25 μL) of 10mM MGO stock and water. To these samples were added 25 μL of 3,4-diaminobenzophenone (DABP, ACROS Organics) from a 20 mM stock in DMF. These samples were incubated at 37 °C and then analyzed via reversed-phase analytical high-performance liquid chromatography using an Agilent Infinity LC system with a mobile phase of water (A) and acetonitrile (B) each containing 0.1% TFA, in which samples were injected onto an AdvanceBio Peptide 2.7 μm column (2.1 x 150 mm², Agilent). Absorbance

spectra at a wavelength of 260 nm were used to detect both unreacted DABP and the addition product between MGO and DABP in each sample. The peak corresponding to the MGO-DABP addition product was then integrated to find peak size.

8. References

- (1) Maillard, L. Action of Amino Acids on Sugars. Formation of Melanoidins in a Methodical Way. *Compte-Rendu Acad. Sci.* **1912**, *154*, 66–68.
- (2) Hodge, J. E. Dehydrated Foods, Chemistry of Browning Reactions in Model Systems. *J. Agric. Food Chem.* **1953**, *1* (15), 928–943. <https://doi.org/10.1021/jf60015a004>.
- (3) Monnier, V. M.; Cerami, A. Nonenzymatic Browning in Vivo: Possible Process for Aging of Long-Lived Proteins. *Science* **1981**, *211* (4481), 491–493. <https://doi.org/10.1126/science.6779377>.
- (4) Yatscoff, R. W.; Tevaarwerk, G. J.; MacDonald, J. C. Quantification of Nonenzymically Glycated Albumin and Total Serum Protein by Affinity Chromatography. *Clin. Chem.* **1984**, *30* (3), 446–449. <https://doi.org/10.1093/clinchem/30.3.446>.
- (5) Tessier, F. J. The Maillard Reaction in the Human Body. The Main Discoveries and Factors That Affect Glycation. *Pathol. Biol.* **2010**, *58* (3), 214–219. <https://doi.org/10.1016/j.patbio.2009.09.014>.
- (6) Richard, J. Mechanism for the Formation of Methylglyoxal from Trisephosphates. *Biochem. Soc. Trans.* **1993**, *21*, 549–553. <https://doi.org/10.1042/bst0210549>.
- (7) Thornalley, P. J. The Glyoxalase System in Health and Disease. *Mol. Aspects Med.* **1993**, *14* (4), 287–371. [https://doi.org/10.1016/0098-2997\(93\)90002-U](https://doi.org/10.1016/0098-2997(93)90002-U).
- (8) Lee, J.; Song, J.; Kwon, K.; Jang, S.; Kim, C.; Baek, K.; Kim, J.; Park, C. Human DJ-1 and Its Homologs Are Novel Glyoxalases. *Hum. Mol. Genet.* **2012**, *21* (14), 3215–3225. <https://doi.org/10.1093/hmg/dd5155>.
- (9) Ahmed, N.; Thornalley, P. J.; Dawczynski, J.; Franke, S.; Strobel, J.; Stein, G.; Haik, G. M. Methylglyoxal-Derived Hydroimidazolone Advanced Glycation End-Products of Human Lens Proteins. *Invest. Ophthalmol. Vis. Sci.* **2003**, *44* (12), 5287–5292. <https://doi.org/10.1167/iovs.03-0573>.
- (10) Chaplen, F. W. R.; Fahl, W. E.; Cameron, D. C. Evidence of High Levels of Methylglyoxal in Cultured Chinese Hamster Ovary Cells. *Proc. Natl. Acad. Sci.* **1998**, *95* (10), 5533–5538. <https://doi.org/10.1073/pnas.95.10.5533>.
- (11) McEwen, J. M.; Fraser, S.; Guir, A. L. S.; Dave, J.; Scheck, R. A. Synergistic Sequence Contributions Bias Glycation Outcomes. *Nat. Commun.* **2021**, *12* (1), 3316. <https://doi.org/10.1038/s41467-021-23625-8>.
- (12) Ramasamy, R.; Yan, S. F.; D'Agati, V.; Schmidt, A. M. Receptor for Advanced Glycation Endproducts (RAGE): A Formidable Force in the Pathogenesis of the Cardiovascular Complications of Diabetes & Aging. *Curr. Mol. Med.* **7** (8), 699–710.
- (13) Batkulwar, K.; Godbole, R.; Banarjee, R.; Kassar, O.; Williams, R. J.; Kulkarni, M. J. Advanced Glycation End Products Modulate Amyloidogenic APP Processing and Tau Phosphorylation: A Mechanistic Link between Glycation and the Development of Alzheimer's Disease. *ACS Chem. Neurosci.* **2018**, *9* (5), 988–1000. <https://doi.org/10.1021/acschemneuro.7b00410>.
- (14) Knörlein, A.; Xiao, Y.; David, Y. Leveraging Histone Glycation for Cancer Diagnostics and Therapeutics. *Trends Cancer* **2023**, *9* (5), 410–420. <https://doi.org/10.1016/j.trecan.2023.01.005>.

- (15) Nemet, I.; Vikić-Topić, D.; Varga-Defterdarović, L. Spectroscopic Studies of Methylglyoxal in Water and Dimethylsulfoxide. *Bioorganic Chem.* **2004**, *32* (6), 560–570. <https://doi.org/10.1016/j.bioorg.2004.05.008>.
- (16) Kellum, M. W.; Oray, B.; Norton, S. J. A Convenient Quantitative Synthesis of Methylglyoxal for Glyoxalase I Assays. *Anal. Biochem.* **1978**, *85* (2), 586–590. [https://doi.org/10.1016/0003-2697\(78\)90258-0](https://doi.org/10.1016/0003-2697(78)90258-0).
- (17) Königstein, J.; Federonko, M.; Alföldi, J. Deuteration of Simple α -Dicarbonyl Compounds and Their Quinoxaline Derivatives. *Chem. Zvesti* **1979**, *33* (4), 515–520.
- (18) Riley, H. L.; Morley, J. F.; Friend, N. A. C. 255. Selenium Dioxide, a New Oxidising Agent. Part I. Its Reaction with Aldehydes and Ketones. *J. Chem. Soc. Resumed* **1932**, No. 0, 1875–1883. <https://doi.org/10.1039/JR9320001875>.
- (19) Shah, C. P.; Dwivedi, C.; Singh, K. K.; Kumar, M.; Bajaj, P. N. Riley Oxidation: A Forgotten Name Reaction for Synthesis of Selenium Nanoparticles. *Mater. Res. Bull.* **2010**, *45* (9), 1213–1217. <https://doi.org/10.1016/j.materresbull.2010.05.013>.
- (20) Brum, V. C. Synthesis of Methylglyoxal-L4C. *J. Pharm. Sci.* **1966**, *55* (3), 351–352. <https://doi.org/10.1002/jps.2600550319>.
- (21) Clelland, J. D.; Thornalley, P. J. Synthesis of ^{14}C -Labelled Methylglyoxal and S-D-Lactoylglutathione. *J. Label. Compd. Radiopharm.* **1990**, *28* (12), 1455–1464. <https://doi.org/10.1002/jlcr.2580281215>.
- (22) Rabbani, N.; Thornalley, P. J. Measurement of Methylglyoxal by Stable Isotopic Dilution Analysis LC-MS/MS with Corroborative Prediction in Physiological Samples. *Nat. Protoc.* **2014**, *9* (8), 1969–1979. <https://doi.org/10.1038/nprot.2014.129>.
- (23) Shishmarev, D.; Kuchel, P. W.; Pagès, G.; Wright, A. J.; Hesketh, R. L.; Kreis, F.; Brindle, K. M. Glyoxalase Activity in Human Erythrocytes and Mouse Lymphoma, Liver and Brain Probed with Hyperpolarized ^{13}C -Methylglyoxal. *Commun. Biol.* **2018**, *1* (1), 1–8. <https://doi.org/10.1038/s42003-018-0241-1>.
- (24) Glomb, M. A.; Nagaraj, R. H. Protein Modifications by Glyoxal and Methylglyoxal During the Maillard Reaction of Higher Sugars. In *The Maillard Reaction in Foods and Medicine*; O'Brien, J., Nursten, H. E., Crabbe, M. J. C., Ames, J. M., Eds.; Woodhead Publishing Series in Food Science, Technology and Nutrition; Woodhead Publishing, 2005; pp 250–255. <https://doi.org/10.1533/9781845698447.7.250>.

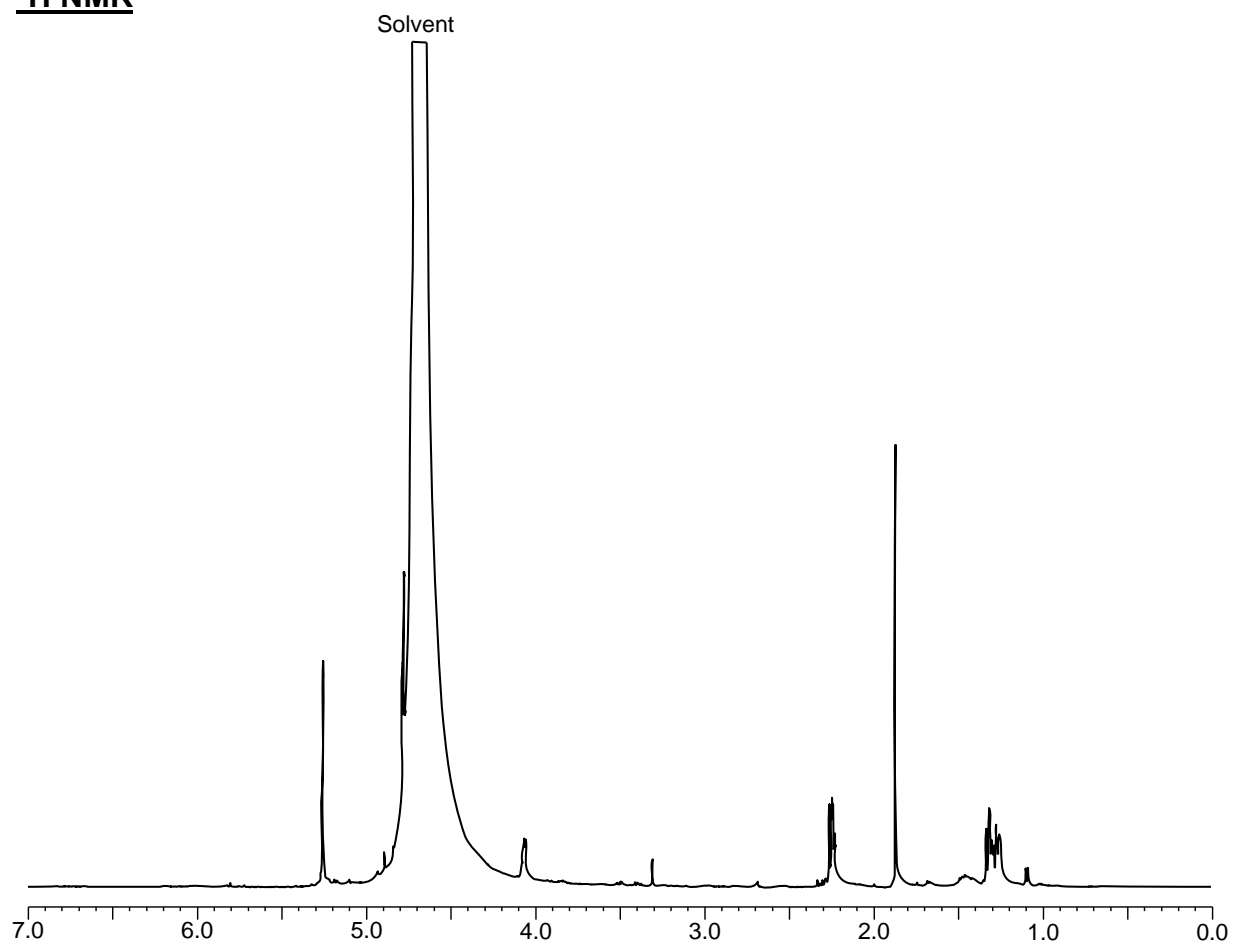
9. Appendix

Tautomerization Reaction without Salt Purification

Appendix 1. Calculation of Salt Concentration.

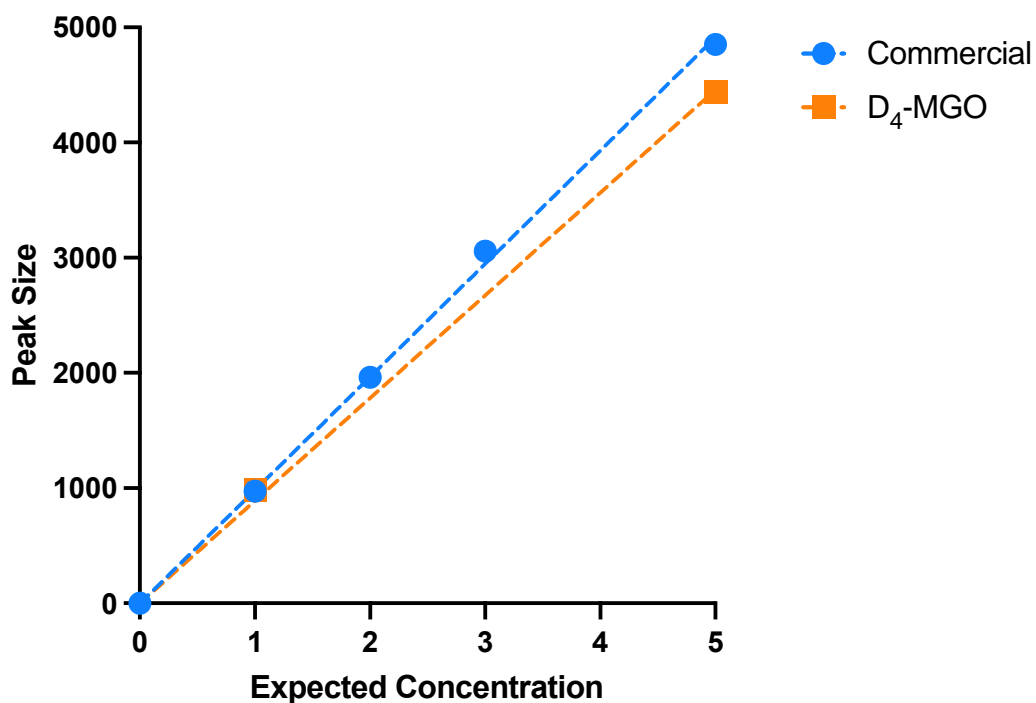
Recent tautomerization experiments which do not purify salt from the use 8 mmol of MGO and 15 mmol of NaCl in a volume of 6mL after neutralization. In glycation reactions, MGO at 1 mM is used. Since the ratio of MGO : NaCl must remain the same at 8 : 15, this puts NaCl at a concentration of 1.9mM in a volume of 50 μ L, resulting in the 95 nmol of NaCl in the reaction. 100 mM (10x) PBS contains 1.37 M NaCl, and in glycation, 20 mM (2x) PBS is used, containing 0.274 M NaCl in a volume of 50 μ L, resulting in 13.7 μ mol of NaCl in the reaction. Therefore, the salt concentration in the MGO is negligible in glycation reactions, as the amount of NaCl added in the MGO solution is over 100 times less than the amount of NaCl added by PBS.

¹H NMR



Appendix 2. NMR of Initial d₃-MGO Synthesis Attempts. First attempts at d₃-MGO synthesis without purification yielded these NMR results with peaks difficult to explain. However, it was determined that these peaks were likely the cause of using commercial MGO as a reagent, which was shown to be less pure than synthetic MGO (Fig. 9). Additionally, when MGO was used in glycation reactions, it appeared to be d₂-MGO, especially when considering the aforementioned issues with neutralization. As mentioned, the protocol has been modified to use synthetic MGO as a starting material, and use NaOD in D₂O to avoid complications during neutralization

DABP Assay of d4-MGO



Appendix 3. DABP Assay of d4-MGO. Due to lower total glycation of d4-MGO (Fig.13), the concentration of the d4-MGO stock solution was analyzed. Error bars are shown but too small to be visible. Using the linear regression of commercial MGO, the actual concentration of the d4-MGO stock solution was calculated to be around 10% less than expected.